Chem Soc Rev

Incorporating Single Molecules into Electrical Circuits. The Role of the Chemical Anchoring Group

Journal:	*Chemical Society Reviews*
Manuscript ID:	CS-REV-07-2014-000264.R2
Article Type:	Review Article
Date Submitted by the Author:	31-Jul-2014
Complete List of Authors:	Leary, Edmund; IMDEA Nanoscience, La Rosa, Andrea; Facultad de Quimica, Departamento de Quimica Organica Gonzalez , M. Teresa ; IMDEA-Nanoscience, Bollinger, Gabino; Universidad Autonoma de Madrid, Departamento de Física de la Materia Condensada Módulo 3 Agrait, Nicolas; Universidad Autonoma de Madrid, Departamento de Física de la Materia Condensada Módulo 3 Martin, Nazario; Facultad de Quimica, Departamento de Quimica Organica

Journal Name

RSCPublishing

ARTICLE

Incorporating Single Molecules into Electrical Circuits. The Role of the Chemical Anchoring Group

Cite this: DOI: 10.1039/xoxxooooox

Edmund Leary,[a,c,*] Andrea La Rosa,[b] M.Teresa González,[a] Gabino Rubio-Bollinger,[c] Nicolás Agraït[a,c] and Nazario Martín[a,b,*]

Received ooth January 2012,
Accepted ooth January 2012

DOI: 10.1039/xoxxooooox

www.rsc.org/

Constructing electronic circuits containing singly wired molecules is at the frontier of electrical device miniaturisation. When a molecule is wired between a pair of electrodes, the two points of contact are determined by the chemical anchoring groups, located at the ends of the molecule. At this point, when a bias is applied, electrons are channelled from a metallic environment through an extremely narrow constriction, essentially a single atom, into the molecule. The fact that this is such an abrupt change in the electron pathway makes the nature of the chemical anchoring groups critically important regarding the propagation of electrons from the electrode across the molecule. A delicate interplay of phenomena can occur when a molecule binds to the electrodes, which can produce profound differences in conductance properties depending on the anchoring group. This makes answering the question "what is the best anchoring group for single molecule studies" far from straight forward. In this review, we firstly take a look at techniques developed to 'wire-up' single molecules, as understanding their limitations is key when assessing a molecular wire's performance. We then analyse the various chemical anchoring groups, and discuss their merits and disadvantages. Finally we discuss some theoretical concepts of molecular junctions to understand how transport is affected by the nature of the chemical anchor group.

1. Introduction

The great attraction with "Nanoscience" and "Nanotechnology" lies in the potential to control matter at its most fundamental level. The logical limit of this involves the manipulation of individual atoms into specific arrangements in order to obtain particular desired properties. In the branch of Nanoscience known as Molecular Electronics, the drive is to fabricate electronic devices in which the active elements, transistors, diodes and switches for example, are built from individual molecules. Using the vast chemistry toolkit it is possible to construct almost any structure. The ability, however, to incorporate the molecules into a circuit in a similarly atomically precise way, one at a time in a controlled fashion, is the crucial aspect that has yet to be mastered. This problem has, perhaps, proven the critical stumbling block of the subject and lies at the heart of problems concerning experimental reproducibility.

A 'chemical anchoring group' can be defined as an atom, or group of atoms, placed at each end of a molecular wire, having good affinity for the electrode material in order to bind the molecule to the electrodes such that transport takes place primarily *through* the molecule. It is sometimes feasible that the electron pathway can bypass the atoms of the anchor group, however the groups should at least orient the molecule in such a way that the major transport is through the molecule. A schematic representation of a single molecule junction is shown in Figure 1. In the simplest case, the key components of the molecule are the functional unit, the part of the molecule expected to behave as a wire, resistor or switch, and the anchoring groups, which are normally placed at the termini of the wire. Additionally, a spacer unit can be incorporated to separate the functional unit from the ends of the molecule for better control via, say, a third, gating, electrode.[1] In this review we shall mainly restrict the discussion to experiments and theory using gold as the electrode material. Although other materials have been explored, such as silver,[2] indium tin oxide[3] and, more recently, graphene,[4] which are worthy studies in their own right, they represent a minority part of the work devoted to studying the molecular binding.

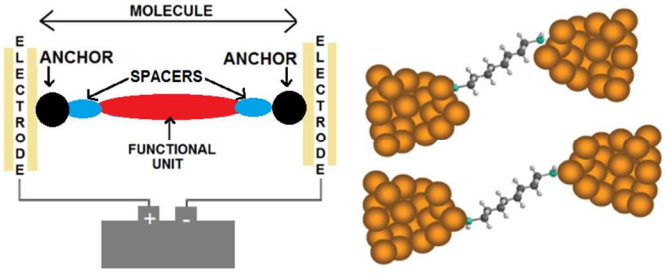

Figure 1. (Left) A schematic representation of a single molecule junction highlighting the key components, namely the anchor groups, a functional unit, spacers (alkyl chains for example) and the enclosing electrodes. (Right) More realistic representations of a junction showing different atomic configurations of the binding to the electrodes.

The main experimental techniques designed to 'wire-up' individual molecules, which have been developed over the past decade, in the main rely on the probabilistic formation of molecular junctions over many repeated attempts. This methodology has allowed insights into many structure-property relationships, such as how the conductance varies with molecule length,[5 6] conformation,[7 8] degree of conjugation,[9] metal complexation[10 11] and redox state.[1 12] There are, however, some major drawbacks to forming junctions in such a spontaneous fashion, which can be viewed as a form of self-assembly. It turns out to be very difficult to control the molecule|electrode interface, particularly in terms of the shape of the electrodes and the precise coordination of the molecule. When a molecule binds, it can do so in many different geometries, related to the shape of the nano-electrodes as highlighted in Figure 1, which shows just a couple of potential binding arrangements. This is believed to be one of the main reasons for the strong conductance fluctuations generally observed from junction to junction, and indeed as an individual junction is stretched. Another factor which leads to conductance fluctuation is the lack of fine control of the number of molecules in a single junction. It is reasonable to assume that the probability of having a two or three molecule junction is similar to that of a single molecule junction. Together, these factors ultimately lead to a broad distribution of measured conductance values, typically more than one order of magnitude, and makes comparing the properties of different molecules somewhat problematic. A reproducibly broad distribution is not fundamentally detrimental for a good comparison, but it is very rarely the case to find such a high level of reproducibility in single molecule experiments. This can perhaps be traced to the difficultly in generating the same distribution of binding geometries and molecular surface coverage in each experiment.

The terminal chemical anchor groups can, however, be easily varied to study their general influence on conductance and binding propensity. This provides us a handle with which to control the contact between molecule and electrode. Varying these groups allows us to probe the transport effects of weak and strong binding, and also mono and multidentate modes of binding, as we shall elaborate on in Section 3. Learning to control this key part of the junction will bring us closer to a fully atomically engineered single molecule device. Before we discuss this any further, we shall first review the main techniques of wiring single molecules, which is important for understanding the way in which the anchor groups behave in the various experiments, and why some groups may be better suited than others depending on the measurement method.

2. Contacting Individual Molecules

There are, at present, several basic ways of trapping individual molecules between a pair of metallic electrodes and measuring the conductance. The methodology is different to that used to assess the conductance of self-assembled monolayers (SAMs), which predates single molecule studies.[13] To investigate the individual molecule regime, the focus is on creating electrodes with dimensions of just a few nanometers, and a separation of similar proportions. This is often done by utilising the tip and the surface of a scanning tunnelling microscope (STM)[14 15] or a conductive atomic force microscope (AFM),[16] or indeed by breaking a thin metallic wire using a mechanically controllable break-junction (MCBJ).[17] In all methods it is necessary to apply a bias voltage between the two electrodes, usually in the range of 0.1 to 0.5 V. Such low voltages are preferable for the BJ technique to avoid high electric fields due to the narrow gap created (e.g. if V = 0.5 V and z = 0.5 nm, the field is $1x10^{10}$ V/m). Higher voltages can be achieved at larger inter-electrode spacings. Generally speaking, there is no limitation on the environment in which measurements can be performed, for example vacuum,[18] air[19 20] and various liquids such as organic solvents[14 21], aqueous electrolyte[15 22] and ionic liquid[1] have all been used, although there are growing numbers of accounts where the environment is considered to influence the experiment.[23 24]

In each method it is assumed there is a finite probability that molecules will bridge the gap between each electrode and that the gap can be varied without the molecule becoming detached. A robust link between the molecules and the electrodes is vitally important as these techniques are typically blind in nature, and to identify the presence of a molecule the conductance of the junction is commonly monitored as a function of electrode displacement. If a molecule becomes chemically bound then a plateau in conductance is usually observed as the junction is elongated (see Figure 3). It is also possible to look for particular features in current-voltage (IV) traces, such as Coulomb blockade or vibrational (elastic tunnelling) events to identify the presence of a molecule. A combination of both forms of analysis is optimal as IV traces give information about the electronic structure of the junction, such as the level alignment, but conductance-distance traces yield information about the geometry of the junction and confirm whether the molecule is physically bound to *both* electrodes. In a growing number of experiments, prior imaging of the molecules is becoming a key step. This allows specific targeting of isolated molecules, which is a distinct advantage over other procedures as it ensures that multiple molecules do not form the bridge. On the downside, small molecules are difficult to measure in this way at room temperature due to their high diffusion, making large molecules better suited.

We shall now elaborate on the principle methods to gain a deeper understanding of their merits and limitations. As we shall see the different methods place different demands on the nature of the anchor group.

2.1 Mechanically controllable break junctions.

MCBJs, introduced in 1985 by Moreland and Elkin, who coined the term '*break junction*', use a thin metal wire mounted on top of a bendable substrate which can be repeatedly broken and reformed.[25] The substrate, typically a phosphor bronze, is mounted to a central piezo stack and two fixed side counter supports. The wire is broken by moving the piezo up, causing the substrate to bend and the wire to stretch until breakage. To reform the junction the piezo is moved downwards. A distinct advantage of MCBJs is that the metal wire can be cooled to cryogenic temperatures intact, and subsequently broken under the conditions of cryogenic vacuum. This creates a clean fracture surface which, coupled with the precise positioning of both sides of the junction, means measurements can be easily performed in the absence of contamination. Another unique aspect of MCBJs is their vibrational stability, which is of the order 10^{-4} nm and is a consequence of the short mechanical path between the two sides of the junction. This is upwards of two orders of magnitude more stable than an STM. Further enhancement of the mechanical stability can be achieved by using e-beam lithography to define the metallic wire.[26]

Muller *et al.*[27] and Van Ruitenbeek *et al.*[28] first employed non-brittle materials like gold to form contacts. This work paved the way not only for the application of MCBJs towards molecular electronics, but also subsequent STM-based techniques. The first BJ experiment carried out with molecules was reported in 1997 by Reed et al.[17] In

their pioneering study, they coated the electrodes with 1,4-benzenedithiol and pushed them together to form a metal|molecule|metal sandwich, demonstrating for the first time the feasibility in studying nanoscale molecular junctions. Kergueris et al. carried out a similar investigation using 2,2':5':2''-terthiophene-5,5''dithiol.[29] They found asymmetric current-voltage (IV) curves, which they attributed to the presence of low numbers of molecules within the junction. This idea was pursued further by Weber et al. who compared a symmetric and asymmetric molecule which, they hypothesised, should give symmetric and asymmetric IV traces respectively.[30] They did find such behaviour, which seemed to confirm the low number of molecules in such junctions. However, as Kergueris showed, asymmetric IVs were obtainable for symmetric molecular structures. This means that from analysis of IV curves alone, one cannot infer purely *single molecule* junctions.

MCBJs, in comparison with STMs, have certain particular drawbacks that favour the STM in several aspects. In particular, MCBJs require an elaborate preparation, and to change the electrodes involves making a completely new device. An STM, on the other hand, is designed for easy replacement of both the tip and the surface, meaning one can be changed independently of the other if there is a problem. Having two electrodes with narrow tips makes it harder to obtain the desired coverage of molecules in an experiment. An STM, on the other hand, has a large, flat, surface which allows many different regions to be explored. Several other factors, including slower electrode separation speeds and uncertainties in stretching lengths, further detract from their use as the most efficient tool for molecular conductance studies. The versatility of the STM makes this a more effective measurement tool on many levels, as shall be discussed in the following section.

2.2 Scanning probe based methods

2.2.1 Molecular STM break junction method. The most abundant technique for creating single molecule junctions is the STM break junction (STM-BJ), demonstrated by N. J. Tao and collaborators in 2003, in which the tip of an STM is driven in and out of contact with a gold substrate covered in molecules (Figure 2).[14] Gold is ideally suited for these experiments for one major reason: its inertness. The vast majority of metals have, under exposure to the air, a layer of oxide of varying thickness. For single molecule conductance studies, having a layer of uncertain thickness introduces an unknown resistance in the circuit, making it impossible to ascertain a reliable molecular resistance. Gold does not form a natural oxide layer upon exposure to air, but it does show high affinity for thiols, making them an obvious choice to anchor molecules in a robust manner.

In the original experiment the electrodes were immersed in a solution of molecules and the measurements carried out *in situ*. Successful experiments can also be achieved by dip-casting preparation techniques, subsequently working under solvent-free conditions.[19] Once sufficient contact between tip and surface is made, the tip is withdrawn, and the measured current (*I*), or more

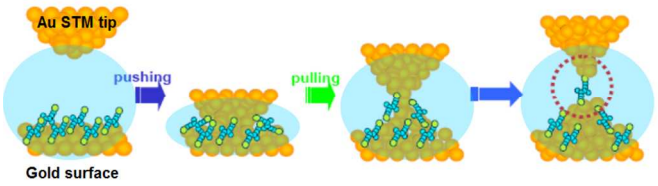

Figure 2. Schematic representation of the molecular STM-breakjunction technique (also applicable to the MCBJ technique).

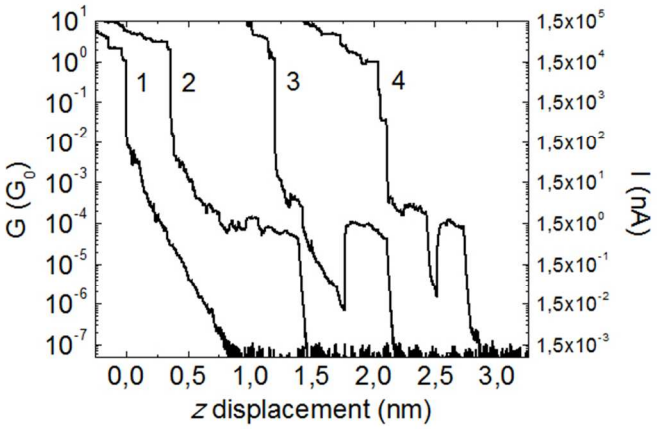

Figure 3. Typical conductance traces from the BJ method shown offset in *x*. For reference, the current (*I*) is displayed on the right hand *y*-axis. Trace 1 shows the typical conductance profile in the absence of wired molecules, i.e. simple tunnelling. Traces 2-4 all show conductance plateaus representative of molecular junction formation. The molecule used was 4, 4'-bis(mercaptomethyl)biphenyl.

commonly the conductance ($G = I/V$), in units of the conductance quantum G_0 (77.5 μS, $2e^2/h$), is plotted as a function of the distance travelled by the tip (*z*). Plotting *G vs z* generates conductance-distance traces, examples of which can be seen in Figure 3.

The main aspects of these traces can be divided into several parts. Firstly a series of steps are apparent which terminate close to 1 G_0. These are a common feature of all traces (although sometimes they are unobservable due to equipment limitations), and signify the final stages of rupture of the gold-gold junction, which often ends in a single atom. The rupture then causes the sudden generation of a nanoscale gap typically measuring in the region of 4-6 Å. When a molecule is not trapped in the junction, the only transport mechanism is tunneling through the measurement medium (trace 1, Figure 3), which can be vacuum, air or solvent. This takes place directly from electrode to electrode and results in an exponential decay of the conductance with distance, the slope of which is determined by the energetic height of the tunnel barrier, until the noise of the instrument is reached.

When molecules are present in the vicinity of the freshly created electrodes, one or a few may migrate into the junction to bridge the narrow gap. It is at this point that the main charge transport pathway across the junction takes place through (potentially) one molecule. This results in a conductance plateau upon further separation of the electrodes (traces 2-4, Figure 3). The presence of such a plateau in G implies that the molecule provides a relatively constant pathway for the current to travel along and can accommodate the change in inter-electrode spacing by tilting and sliding with respect to the electrodes. In molecular junctions the "plateau" is never very flat however, and may contain sudden jumps, either up or down, and may also possess a gentle overall slope. The reasons for this behavior are invariably difficult to pin down precisely, however, it is normally assumed to be the result of changes in adsorption of the anchor groups, atomic rearrangements of gold atoms due to stress, conformational changes within the molecule and/or addition of other molecules to the junction. Ultimately, the build-up of tensile stress on the junction will cause it to rupture at its weakest point, which is seen as a sudden drop in conductance from the plateau as the system relaxes. The opening and closing cycle is normally repeated many times in order to build a statistic of as many different junctions as possible. For

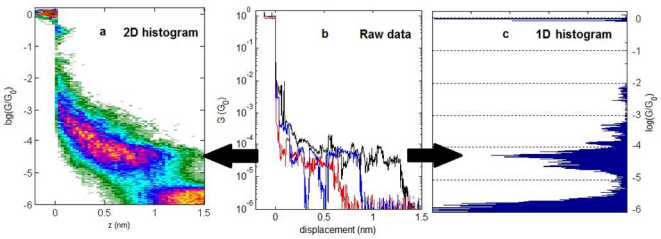

Figure 4. 1D and 2D histogram generation from individual conductance traces of NH_2-OPE3-NH_2, where 3 denotes the number of Ph rings. The 2D histogram contains more traces than shown in b for clarity.

practical reasons the limit of repetitions usually falls in the range of thousands to tens of thousands of cycles.

The standard manner to summarise the recorded traces is to plot histograms of the conductance and the conductance versus distance. This generates *one* and *two*-dimensional histograms (Figure 4c and 4a respectively) which allows the general conductance profile of a compound to be compared with another, and also with other results for the same compound.

The detailed mechanism of how each junction forms in the STM-BJ method usually remains unclear, although some general situations can be envisaged. It is possible that a molecule is already bridging both electrodes, before the gold junction is broken, to the side of the neck. Once established, the molecule can diffuse into the gap whilst remaining anchored. This is assumed to be the situation when the conductance plateau is visible immediately after the gap opens (trace 2, Figure 3). Alternatively, no molecule may be bridging the junction initially, but one may jump into contact after a certain time. This is likely to have happened when an initial exponential decay of the conductance is observed, followed by a jump to a plateau (trace 3, Figure 3). It is also possible that a junction can break and reform during the course of a single measurement. If this happens frequently, it may be an indication of an anchor group's specificity to certain binding sites. The ratio of unbroken (trace 2, Figure 3) to broken (traces 3 and 4, Figure 3) plateaus can potentially yield information on the strength or specificity of binding.[31] On a simple level, one can argue that a weakly bound molecule is expected to detach more frequently than a strongly bound molecule, displaying more broken plateau traces. On the other hand, this idea may not hold for anchor groups which bind preferentially to certain coordination sites, which when pulled may not be able to maintain their preferred binding. Other factors can be expected to play a role in trace profile, such as molecular surface coverage. Wiring more than one molecule, for example, will reduce the probability of observing clear, individual molecule, detachment events.

2.2.2 STM non-contact methodology. Closely related to the molecular STM-BJ technique are the methods developed by Haiss et.al. which are also based also on trapping molecules between the tip and surface within an STM (Figure 5).[15 32] The crucial difference is that contact between tip and surface is avoided. In the 'I_s' technique (I = current, s = distance), the tip is brought into close proximity with the surface using a predetermined set-point current. After waiting, the tip is withdrawn in a similar manner to the STM-BJ method, and by a similar distance. The same statements described above also apply here in determining whether a molecule bridged the gap during the measurement cycle. Here, however, it is assumed that molecules must initially jump between the tip and the surface in order to bridge as no metal-metal contact is formed. The starting tip-surface distance must also be estimated when evaluating the breakdown distance of each junction. To do so, the average barrier height (in eV) must be obtained, however as this may change from point to point on the surface, there is the potential for some uncertainty in absolute distance calibration. This procedure is usually carried out on a surface with a low coverage of molecules to avoid the formation of self-assembled islands or monolayers, which are unlikely to favour single molecule junctions. The flatness of the surface, on the other hand, is preserved, unlike in the BJ method, allowing the structure of at least one of the electrodes to be reasonably controlled. This means that experiments can be performed on flat terraces (ensured by prior imaging) clarifying one of the electrodes (although binding to adatoms is potentially possible). The tip should also have a lower curvature as it is not continually crashed into the surface. These aspects could result in different possible contact geometries between the molecule and the tip, as has been postulated.[32 33] A requirement of the non-contact method is that molecules must spontaneously 'jump' from the surface to the tip through one of their anchor groups. This implies that the anchor (and indeed the molecule) should have a reasonably dynamic interaction with gold.

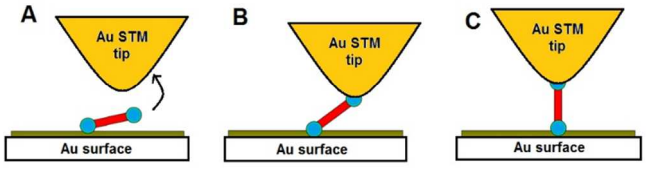

Figure 5. The essential steps in the non-contact STM techniques where the molecule first must jump to contact.

In both methods, STM-BJ and non-contact-STM it is possible to estimate the electrode separation at with the molecular junction breaks down. In the STM-BJ experiment, the point at which the gold junctions break can be used as a reference for calibration. One must estimate the amount of unseen retraction (also known as 'electrode snapback'), which may give an error of roughly 1-2 Å in absolute terms. The comparison of the stretching length with the known length of the molecule allows us to check that we are, for example not wiring multilayers of molecules. It also allows us to be confident that the conductance plateaus are indeed related to the molecules we deposit, and not, perhaps, a contaminant. Both technique rely on the probability that a low number of molecules are found bridging the metal gap. This is usually confirmed by the junction breakdown distance. However, the absolute number is not directly observable, and cannot be elucidated from the conductance or the breakdown distance.

In the early STM studies, multiple conductance peaks with integer spacing were presented, the lowest of which used as evidence of the formation of single molecule junctions.[5 14] Sometimes, non-integer spaced peaks were found, with the explanation that these arise from distinct binding configurations of the anchor groups. This was the case for alkanedithiols, and up to three distinct conductance groups have been seen in individual measurements.[34 33 35] Other studies have, however, failed to find the same behaviour, and instead a single dominant broad peak is observed.[36] The reasons for these different observations are not fully understood, and are normally explained by different discrete binding geometries, different molecular conformations or aggregation of molecules. Another plausible explanation may lie in the different methods of data analysis that are used by each group. As the signature of a molecular junction is open to some interpretation, it is possible for similar data sets to be represented differently by different analysis methods. Indeed, it is possible that data which would be rejected by one method, is included in the final analysis in another. The lack of a

standard way of treating and presenting data can make it hard to compare results from different laboratories. One final factor in the varying numbers of observed conductance values could be the range of conductance explored in each measurement. This depends on the sensitivity of the equipment used.

The implications are profound as to whether multiple molecule junctions can be observed in discrete groups. If it is the case, then it would mean that the influence of the binding group on the conductance is quite low. This would indicate that either different binding sites affects the conductance little, or perhaps that only certain bindings are seen in the measurement. The observation of a broad peak, on the other hand, with a width of about one order of magnitude in the log histogram representation suggests that the effect of the binding of the molecule is relatively large, which therefore should wash out the final observation of multiple molecule junctions.

Despite these experimental concerns, there are examples of high levels of agreement for certain compounds over several methods from several laboratories. A particularly nice example is for the measurement of oligo(phenylene ethynylene) molecules (OPE) with thiol terminal anchor groups. OPE molecules with three benzene rings have been studied independently by several groups using both the STM-BJ,[19 37] non-contact-STM[38] and MCBJ[9 37 39] techniques in ambient and liquid conditions, where very similar conductance histogram profiles have been found in all cases. On the contrary, low temperature experiments have not been as successful in replicating room temperature studies. For example, in an STM-BJ experiment under liquid conditions performed by Venkataraman et.al, 1,4-benzenediamine (BDA) was found to show a much narrower conductance distribution that its thiol counterpart 1,4-benzenedithiol (BDT).[40] This result could not be reproduced by Martin et al. who studied the same two molecules at 77 K using an MCBJ.[41] They found a broad conductance histogram for BDT, and hardly any signal for BDA. Compared to the reference sample in toluene, even the signal of BDT was low. This rather in fact suggests a general difficulty in forming molecular junctions at low temperature using BJs. The number of traces recorded was low in comparison with the STM results, 300 versus 10,000 in the STM study. In the same study, Martin et.al. measured 1,6-hexanedithiol, and found that the histogram peak depended on the amount to which the gold was fused before separation. A large gold-gold contact resulted in suppression of the peak, suggesting that molecular junction formation is, in part, controlled by diffusion of the molecules into the junction. In comparison to the results of Martin, Tsutsui et al. found conductance histograms of BDA similar to that in ref[40] using an MCBJ operating under vacuum at room temeprature.[42] Clearly, therefore, at low enough temperatures, molecular motion becomes frozen, hindering the ability to form junctions via diffusion. It is likely that the mobility is strongly determined by the anchor group, as this is the part of the molecule which interacts the strongest with the electrodes. Hence, at low temperatures, these results suggest that it may be beneficial to use even weaker anchor groups to aid the formation of junctions when applying the BJ technique.

2.2.3 Prior imaging methods. A better way to measure the conductance of only one molecule, as opposed to the previously discussed 'fishing' techniques, is to image an individual molecule before it is contacted. Only in this way can it be agreed that one molecule is studied. Cui et al. developed an innovative approach using a conducting-AFM to contact gold nanoparticles capping alkanedithiol molecules embedded in a matrix of alkanethiols.[16] The nanoparticles sit ontop of only the dithiol molecules, and due to their high dilution, it was assumed this should mainly correspond to individual molecules. The small size of the nanoparticles used (1.5 nm), however, created problems associated with charging effects of the nanoparticle itself. When larger nanoparticles were used, a greater spread of conductance values was found, presumably due to a higher density of dithiols under the nanoparticle.[43] These issues have left this procedure relatively unused.

Pinpointing the location of molecules on a surface is routine using low temperature STM, in which the motion of molecules is frozen, allowing high-resolution images to be recorded before the molecule is contacted. This has been achieved, most notably, by pressing the tip onto individual C_{60} molecules.[44 45 46] Apart from this, relatively few studies have been devoted to studying single molecular wires at low temperature. Notable examples include: a single polyfluorene chain,[47] a single polythiophene chain,[48] a perylenetetracarboxylic dianhydride (PTCDA) molecule[49] and octanethiol.[50] Notably, in each of these examples there is a lack of conventional binding groups at each end of the molecule. Under UHV, it is possible for most atoms to bind to the clean metal surfaces, which are free from contaminants. Under non-UHV conditions, the adsorption energies of physisorbed species, such as these mentioned above, would be much too low and could not compete with other molecules from the atmosphere. Further drawbacks of the low temperature UHV approach lie in the fact that not all molecules are suitable, only those that can be deposited under UHV conditions, or generated in situ from a precursor are viable. This usually rules out large or unstable molecules.

In an attempt to marry the two methodologies of low temperature imaging with the ease of room temperature operation, we have recently introduced an ambient condition approach to the 'targeted wiring' methodology through the use of molecules terminating in C_{60}, known as dumbbells due to their overall shape (Figure 6).[51] These bulky groups prevent significant movement of the molecule across the surface under ambient conditions, allowing the tip to be placed accurately over one of the C_{60} groups. The C_{60} then becomes the anchor group once the molecule is lifted. This procedure will be discussed in more detail in section 3.3. The important result of these measurements was to reveal the variation in conductance produced just by one molecule, which can be directly attributed to the geometry of the molecule in the junction.

Perhaps one of the main drawbacks to room temperature STM

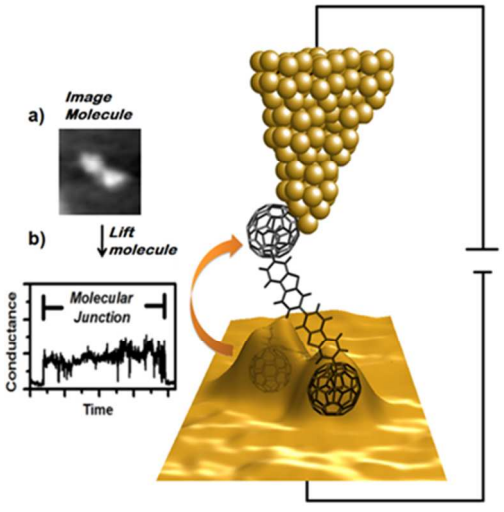

Figure 6. The targeted wiring approach. The image in (a) shows the appearance of the terminal C_{60} groups. The same image is represented in the 3D sketch of the junction. Reprinted with permission from ref 51.

experiments is the inability to form long-lived junctions. This is limited by the stability of the microscope, which under optimal conditions gives a drift of the tip in x-y of about 10 pms^{-1}. This places a limit of about a minute in which the tip remains close to its original position. To carry out studies into the stability of molecular contacts over longer periods, it is preferable to keep the relative position of the electrodes constant. This is achievable by using mechanically controllable break junctions (MCBJs), which we shall now briefly discuss.

3. Chemical Anchoring Groups.

The bonding between a molecule and a metal is weak in comparison with the typical bonds which form the molecule. Compared with covalent bonding, like a carbon-carbon single bond with a bond energy of around 4 eV (92 kcal), a metal-molecule bond is usually weaker, in the range of 0.5 to 2 eV (11.5 to 46 kcal). The ensuing charge transfer between metal and molecule upon binding (potentially in either direction) occurs in order to equilibrate the chemical potential across the junction. This is expected to result in the formation of a dipole at the interface, which should determine the final value of the Schottky barriers, giving rise to the potential to dominate the charge transport characteristics of the junction.[52] For this reason, the nature of the chemical anchor group will strongly influence the amount of charge transfer and the final energy level alignment (i.e. the relative positions of the HOMO/LUMO with the Fermi level). Another aspect influenced by the anchor group is the electronic coupling between the metal and the molecule, which essentially describes the degree of the hybridisation with metal states. In practice, the level alignment and coupling can be determined experimentally.[53] To elucidate the role of the anchor group, systematic studies are needed where the molecule remains the same and only the anchor group is substituted. As we shall see in the following sections, although such studies have been carried out, there is still plenty of room for further, more comprehensive comparisons. Many times, practical reasons dictate the choice of anchoring group, such as ease of chemical synthesis, junction stability and the propensity for conductance fluctuations. Shown in Figure 7 are the chemical structures of a wide range of groups which have been tested to some degree.

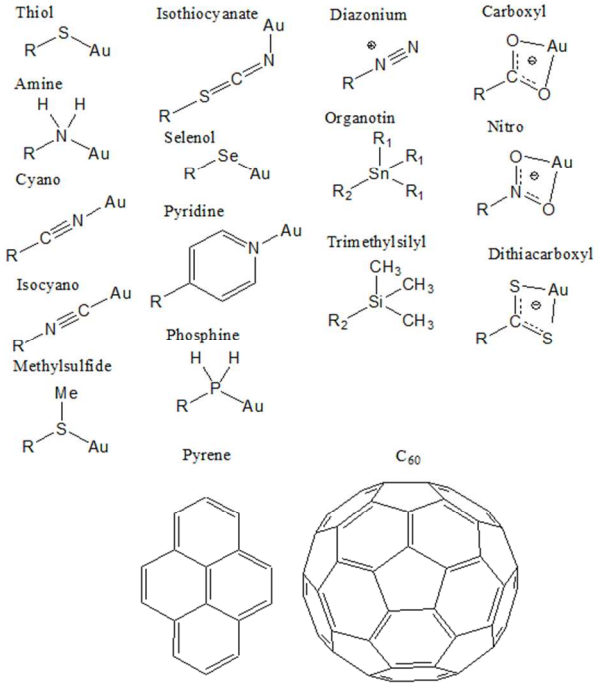

Figure 7. The chemical structures of various anchor groups and their coordination bonding to gold. Note that the diazonium, organotin and trimethylsilyl groups are cleaved upon exposure to gold to form Au-R.

Below we have listed some of the types of anchoring group, along with an example reference. Each group can be classified according to the number of binding atoms:

- Monodentate anchor groups: These bind through one atom only. Examples include; thiol,[17] amine,[54] cyano,[55] isocyanate,[56] isothiocyanate,[57] selenol,[58] pyridine,[59] phosphine,[60] diazonium compounds,[61] organotin compounds[62] and trimethylsilyl protected alkynes.[63 64] It should be noted that the last three examples are all believed to form Au-C bonds.
- Bidentate anchor groups: Two atoms form the contact. They include; nitro compounds,[53] carboxylic acids[65 66 8] and dithiocarboxylic acids.[67]
- Multidentate anchor groups. These include larger groups which can bind through partial or whole facets of the group. The number of atoms involved in the contact is not necessarily defined. This includes C_{60}[68 51 69] and pyrene.[4]

3.1 Monodentate anchoring groups

3.1.1 Gold-sulfur linkage – The archetypal contact

The proto-typical chemical group in single molecule electronics is the thiol, which binds readily with gold surfaces. The gold-sulfur bond is commonplace in many areas of nanoscale research and is widely used to anchor organic and biomolecules to surfaces and is noted for its ability to form ordered self-assembled monolayers (SAMs).[70] Thiols (RSH) are used extensively to cap gold nanoparticles, forming a stabilising shell to protect the nanoparticle. The accepted mechanism of Au-thiol bond formation involves the generation of a thiyl radical (RS•) to form a strong Au-S bond which is considered covalent. In recent years it has become clear that the strength of this bond is responsible for significantly modifying the interface of thiolate-SAMs and thiolate protected gold nanoparticles (GNPs). In the case of thiolate-SAMs, it is normally difficult to elucidate the precise atomic arrangement of the interface. Figure 8 shows some possible binding modes of thiolates to gold.

On the other hand, by means of x-ray crystallography, the atomic structure of certain GNPs is known. The surface of the thiolate-protected nanocluster $Au_{102}(p\text{-MBA})_{44}$, prepared by the "one-phase"

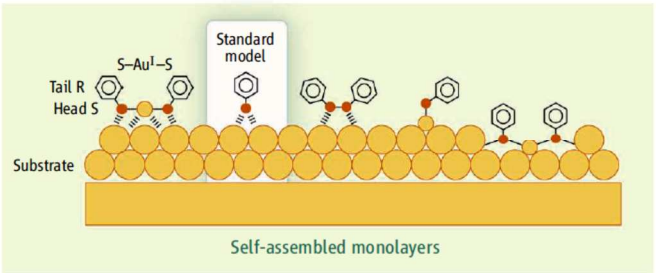

Figure 8. Different proposed binding modes of thiols to a gold surface. Reprinted with permission from ref 151.

method, and where MBA is *p*-mercaptobenzoic acid, has been found to be surrounded by two types of "staple" motifs: RS-Au_{ad}-SR and RS-Au_{ad}-RS-Au_{ad}-SR (ad = adatom).[71] This work showed that the surface of a GNP is not a smooth sphere, as once believed, and brings to the fore the non-trivial nature of the gold-thiol interface. Recent STM images of low coverages of several different thiolates have reinforced the adatom binding picture by observing similar structural motifs as seen in the nanoparticles.[72]

Thiols, in particular aromatic thiols, are known to oxidize readily, and previous work with α,ω-alkanedithiols has suggested that they can form multilayers on gold via disulfide linkages or that they can form ring structures in which both ends of the molecule bind to the surface. Protection of the thiol group is ready achieved in several ways, most commonly via the use of the acetyl protection moiety. This methodology was examined by Tour et al. who studied SAM formation for a whole series of aromatic compounds with thiol and thioacetate terminal groups. They found that the acetate spontaneously cleaves on exposure to gold, allowing SAM formation, and that development of the SAM does not progress beyond a monolayer unless a specific deprotection agent, such as NH_4OH, is added. We have performed BJ studies on acetyl-protected oligophenylene ethynylene (OPE) wires under different environmental conditions. In both solvent and solvent-free conditions, we found the same conductance signature found for the deprotected, free thiol, molecule. However, performing the experiments in the presence of solvent reduced the probability of forming junctions compared to the solvent-free, ambient environment. We attributed this effect to there being a lower amount of water available to cleave the acetyl group under solvent (which was either 1, 2, 4-trichlorobenzene or mesitylene).
There are, of course, many other ways of protecting thiols, all of which, however, require specific deprotection to liberate the thiol on gold. In particular, one strategy which has been shown to allow single molecule junctions without deprotection is by the use of methylsufide termini. The methyl group is not cleaved upon exposure to gold, but is small enough so that the sulfur atom can still coordinate using one of its lone pairs. For alkanes, the results were comparable to the amine linked analogues.

Research with thiols in single molecule studies stems from the early electron transfer studies carried out on SAMs.[73] In these early measurements, thiols were used to bind the molecule strongly to the electrodes, and the backbones were chosen to be structurally uncomplicated, such as simple alkane chains or benzene rings. Such systems were, therefore, the primary target of the first single molecule studies. However, despite their seeming simplicity, a state of disagreement, or perhaps confusion, has existed for many years over whether a well-defined conductance exists for such simple molecules as 1,4-benzenedithiol (BDT) and different length α,ω-alkanedithiols. Throughout the literature, reported values of single molecule conductance of BDT range from approximately 0.5 G_0 to 10^{-4} G_0.[40 74 75 76] In several cases, only one value is quoted, whilst in other studies conductance values are observed over the whole range reported. This is a huge variation if we consider just the conductance of a metal nano-contact, where the spread of values is actually low enough to observe histogram peaks related to junctions with discrete numbers of atoms.[77] A relevant question to ask is whether or not the variation in molecular junction conductance originates from the nature of the Au-S bond, variations of which can be seen in Figure 8, or can it be explained by other experimental factors?

Xu and Tao initially reported conductance values for 1,6-hexanedithiol (HDT) and 1,8-octanedithiol (ODT) of 1.2 x 10^{-3} G_0 and 2.5 x 10^{-4} G_0 respectively using the BJ method.[14] Shortly after, Haiss et. al. reported significantly lower values for the same compounds, 3.2 x 10^{-5} G_0 and 1.3 x 10^{-5} G_0 for HDT and ODT, using the non-contact wiring methods.[32] In a subsequent study using the BJ method, Li et. al. reported an intermediate value for ODT of 5.2 x 10^{-5} G_0 whilst also observing the higher value reported by Xu and Tao.[34] Li et. al. could observe conductance plateaus in the same region as Haiss, but they did not observe a well-defined peak in the conductance histogram.[34] Likewise, using the non-contact approach, the intermediate conductance value of ODT was observed by Leary et.al.[78] In several subsequent studies, all three conductance values have been seen, although the postulated origins differ greatly. Li et.al. proposed that the high and medium values were due to different contact configurations, whilst the low value originated from a gauche defect in the alkane chain.[35] Haiss et.al. proposed that each group corresponded to a different contact configuration, with the higher values relating to higher coordination numbers of the sulfur atom with gold.[33] On the other hand, Gonzalez et.al. suggested that the high conductance group was in fact due to multiple molecules being present in the junction.[79] This was based on the observation that the highest conductance values only appeared when they did not form a gold-gold junction in the opening and closing cycle of the electrodes.

Monitoring the conductance alone, as these studies have done, provides very little information about the mechanics of the contact. In order to obtain a deeper insight, several groups have looked not only at the conductance, but also the force applied to the junction under tension. Xu et.al. used a conducting-AFM to measure the force required to break junctions of ODT. They reported a value of 1.5 nN for junctions with a conductance equal to the high value previously found by the same authors. They attributed this to the breakdown of the junction at one of the Au-Au bonds in the electrodes. The value is very similar to that measured for Au-Au junctions in the absence of molecule,[80] which likely indicates that the Au-S bond is stronger than the Au-Au bond, and that the molecule may pull gold atoms from the electrodes before rupture takes place. In a more recent study, Nef et.al. also measured the breakdown force of ODT junctions, finding the same mean force as Xu.[81] In this study, however, the conductance associated with this breakdown force was 1.1 x 10^{-5} G_0, i.e. in accord with the lowest reported conductance for this molecule. Both studies, therefore, indeed seem to be measuring the breakdown of molecular junctions, but the details of how the molecule is bound to the gold, it's coordination, and the number of wired molecules is still illusive. Nef argued that below 10^{-5} G_0, there was a sharp cut-off in forces up to 1.5 nN, suggesting at least that this conductance is likely to correspond to a single molecule.

Another way to test if the spread in conductance arises purely from the nature of the Au-S bond is to substitute the thiol anchor for other groups, such as amines, which may bind in a different manner. This idea was proposed by Venkataraman et.al.[40] who studied junctions formed by lone-pair interactions with gold. This will be discussed in the next section.

3.1.2 Gold interaction with lone pair atoms

Apart from amines, this category includes several groups containing N atoms such as pyridine and nitrile. Other p-block elements can be successfully used too, in particular S, Se and P. Amines were the first of this type tested and it was hypothesised that they would bind in a less complicated manner than thiols, hence reducing the spread in conductance values.[40] Amines are well-known as ligands which

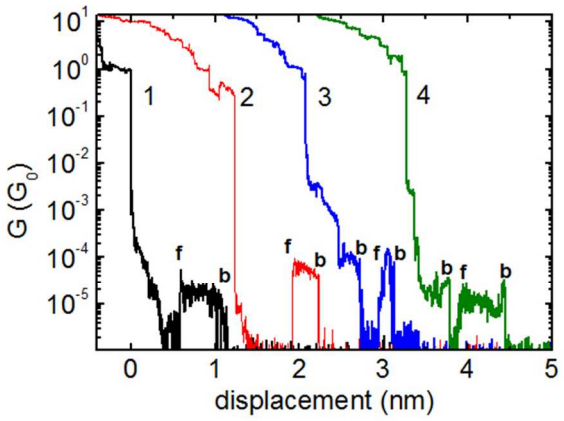

Figure 9. Typical conductance versus distance traces for amine terminated OPE molecules. The conductance can vary over approximately one order of magnitude. The letters f and b denote junction formation and breakage respectively.

bind to a wide variety of metal centres in coordination complexes. They sit in the middle of the spectrochemical series (which describes the degree of splitting between metal centred bonding and anti-bonding states upon ligand coordination) due to their weak donor/acceptor properties. To prove the efficacy of this group, Venkataraman et.al. looked at the length dependence of the conductance for a range of amine terminated compounds, including alkanes[40] and oligo(phenyl)s[82] amongst others. In the case of alkanes ranging from 1, 2-ethylenediamine (C2) to 1, 12-dodecanediamine (C12) a beta (β) decay constant of 0.76 ± 0.01 $Å^{-1}$ (0.97 ± 0.02 per methylene group) was found, which is consistent with an off-resonant tunnelling mechanism and fully in-line with value found from numerous other studies. The beta value is a measure of how the conductance is attenuated by increasing the length of the molecular backbone in a simple tunnelling picture.[83] For the series of oligo(phenyl) compounds with 1, 2 and 3 rings, a decay constant of 0.43 ± 0.02 $Å^{-1}$, or 1.8 ± 0.1 per phenyl ring, was found. This also agrees with previous measurements, and fits with the expectation that oligo(phenyl)s should have a lower β factor than alkanes due to their smaller HOMO-LUMO gaps and pi-conjugation.

In a breakjunction study by Arroyo et.al. amine and thiol anchor groups were directly compared for various length alkanes to highlight their differences.[36] One of the main aspects which change when thiols are substituted by amines in these molecules is the behaviour of the gold electrodes. Amines were seen not to modify the gold breaking dynamics significantly with respect to unmodified gold, evidenced by the normal gold jump-out-of-contact and junction separations at breakdown comparable with the length of the molecule. On the other hand, the thiol terminated alkanes, strongly modified the gold breaking dynamics. This resulted in junctions with apparent stretching distances significantly longer than the corresponding amines and, indeed, the molecular length, indicating mobilisation of gold atoms in the contact. Another observation was the ability of alkanes to self-assemble inside the junction. The junctions with the longest stretching lengths were also those with the highest conductance, and this was interpreted as due to more molecules participating in these junctions. Conversely, for the amine junctions, the same trend was not apparent, and the conductance was much more constant over the length of the plateaus. The overall result was that alkanedithiols gave a larger spread in conductance values, although how much of this is due to the uncontrolled number of molecules in each junction remains unclear. Alkanediamines, it was concluded, are more likely to form junctions with fewer molecules.

Gonzalez et.al. studied an amine terminated OPE molecular wire and found that junctions could be grouped into two main categories based on the plateau profile of a molecular junction.[31] Two main profiles were observed, those with uninterrupted, continuous, plateaus from beginning to end, and those with a drop in conductance below the noise level which persisted for a certain duration, termed 'broken' plateaus. Examples of such 'broken' plateaus can be seen in Figure 9, where the formation (f) of the junction and the breakage (b) have been labelled. In terms of the conductance spread, this varies upwards of one order of magnitude along a plateau and from junction to junction. 1D and 2D histograms can be found in reference.[31] The junctions showing continuous plateaus generally were found to have a higher conductance, whilst the opposite was true for the 'broken' plateau traces. The combination of a slightly lower conductance and the 'on-off' junction behavior suggests that these junctions more likely contain single molecules than the junctions with uninterrupted plateaus. Alternatively, without assuming differing numbers of molecules, it could be that such junctions actually involve a weaker bound molecule, whilst in the continuous junctions the molecule is more strongly bound. Contrary to this explanation, however, is the observation that the total stretching length of the junctions in both cases was very similar, with the broken-plateau junctions in fact surviving slightly larger electrode separations. The opposite behaviour would be expected if the binding is weaker. The length of the plateaus was also measured at differing electrode separation rates, and the main outcome was that the length did not vary significantly over the range studied (0.1 to 100 nms^{-1}). This shows that for amines, the lifetime for thermally induced desorption must be larger than the slowest measurement time (a few seconds), and junction breakages observed in the experiment are always produced by the displacement of the electrodes, which is suggestive of binding specificity.

There are several theoretical studies into the binding and conductance properties of amine linked molecules to gold. The general finding is that amines prefer to bind to under-coordinated atoms, showing higher binding energy than on flat surfaces.[53 84] In terms of the chemistry of amine terminal groups, the lone pair on the N atom has a different reactivity depending on whether the amine is attached to saturated groups such as alkanes, or conjugated groups such as benzene. In the case of aromatic amines, the lone pair is conjugated with the pi-electron system, with the result that aromatic amines are generally weaker bases than aliphatic amines. The pKa value for the conjugate acid of aniline (Ph-NH_2) is around 5, in contrast to values above 10 for aliphatic amines. The pKa value is a measure of the reactivity of electron pairs towards a proton, the higher the value, the higher the binding strength. It should provide a reasonable estimate to the binding strength of a particular group with a metal on the basis of a simple donor-acceptor picture. This can of course be different for metals, which have a variety of orbital shapes and can back-donate charge depending on orbital symmetry.

Regarding the binding to a metal, the difference in reactivity between conjugated and non-conjugated lone pairs should have some influence on the strength of the resultant bond. Only a few studies have actually been undertaken to assess the binding strength of molecules to electrodes, which requires the simultaneous measurement of the conductance and force required to break the junction. One study has performed such a comparison between aromatic and aliphatic amines, specifically 1,4-benzenedimane and

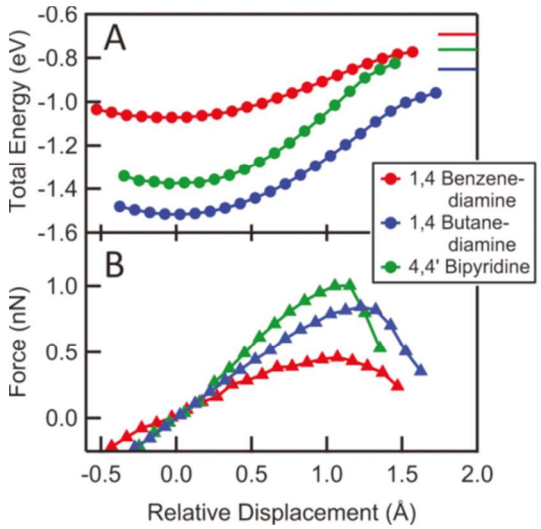

Figure 10. (A) Calculated total energy curves for 1,4-benzenediamine (red), 1,4-butanediamine (blue) and 4,4'-bipyridine (green) as a function of electrode displacement. (B) Calculated displacement-force curves. Reprinted with permission from ref 85.

1,4-butanediamine. In this study, Frei et.al. found that the mean force required to break junctions of 1,4-benzenediamine was 0.53 nN, whist 0.69 nN were required for the junctions of 1,4-butanediamine.[85] This behaviour fits with the simple expectation based on the basicity of the free molecules. Interestingly, the same study measured the force required to break junctions of 4,4'-bipyridine, where the N atom is part of the six-membered ring, contributing to the pi-system. The measured force for such junctions was found to be 0.80 nN, higher than the amine junctions. Despite the lone pair of pyridine being orthogonal to the pi-system, and hence formally not being in conjugation with the ring system, the basicity of pyridine is still similar to aromatic amines. In order to explain the slightly higher than expected bond rupture force values, it was proposed that pyridine also involves a contribution to the binding from the pi-system itself (i.e. via one face of a pyridine ring). Theoretical calculations (Figure 10) support the experimental findings, confirming that aromatic amines bind more weakly than aliphatic amines.

The same group has shown, however, that binding strength is not particularly related to conductance. Despite the higher binding strength of 4,4'-bipyridine, the conductance of the structurally similar 4,4'-diaminobiphenyl is in fact higher. This is also despite the shorter overall length of bipyridine. A similar finding from theory was reported by Zotti et.al.[53] Two conductance histogram peaks of 4,4'-bipyridine were found by Venkataraman et al., $5x10^{-4}$ G_0 and $2x10^{-4}$ G_0,[86] both values being lower than that reported for 4,4'-diaminobiphenyl of $1x10^{-3}$ G_0. This suggests that the conjugation of the lone pair in the biphenyl molecule outweighs the shorter N-N distance in bipyridine in terms of molecular conductance. Widowski et.al. compared the junction thermopower of 4,4′-diaminostilbene (amine anchors) to that of 1,2-di(4-pyridyl)ethylene (pyridine anchors).[87] The thermopower of a junction[88] gives a direct measurement of the value of the slope of the transmission at the Fermi level, including the sign of the slope. They found that the diamine gave positive values for the Seebeck coefficient (S), indicating transport dominated by the HOMO, whilst the pyridine compound showed negative S values, corresponding to LUMO transport. This highlights an important role played by the anchor group, namely that they can control the level alignment within a junction, essentially determining the principle charge carriers (holes or electrons).

As previously mentioned, pyridine terminated molecules are generally found to show more than one conductance group. One particular molecule, which has been studied by several groups, is 1,2-di(4-pyridyl)ethyne. Martin et.al. have reported three groups of conductance,[89] Garcia also report three,[90] whilst Velizhanin report only two.[91] Confusingly, the three values found by Martin are not exactly the same as those of Garcia, the middle and lower groups of Martin agrees the higher and middle groups found by Garcia respectively. In other words Martin et.al. find an even higher value than Garcia. Quek et.al report two conductance values of the slightly shorter 4,4'-bipyridine,[86] whilst Martin et.al. again find three. The relevant question here is how is a particular conductance group defined? This is beyond the scope of the review to answer this question, but it seems reasonable, given the number of studies reporting a large spread in conductance groups, that the least we can assume is that pyridine anchored molecules bind to gold in a variety of ways, which produces a large variation in junction conductance. Interestingly, Velizhanin et.al. reported that the molecule perfluoro-1,2-bi(4-pyridyl)ethyne gave only one conductance group, which was similar in value to the low conductance group of the non-fluorinated compound, also measured by Martin and Garcia. They reasoned, therefore, that the larger fluorine atoms must sterically hinder the pi-system of the pyridine from interacting with the gold, which hints at a plausible origin of the large spread in conductance values.

As for other groups which bind through N-based lone pairs, cyano groups, also known as nitriles (R-CN), have been analysed in several studies.[55 90 92] A junction formation probability of 60 % has been observed in the case of cyano-terminated diaryloligoynes,[90] which is similar to the percentages found for structurally similar OPE diamine junctions.[31] From the chemical perspective, nitriles should form weaker bound junctions due to their low basicity, the pKa is circa -10 for the conjugate acid R-CN-H^+. As far as we know, no study measuring the breakdown force of cyano terminated junctions has been undertaken. Theoretically, though, the binding energy of such junctions has been calculated, and the energy for the most stable junctions in the case of a series of tolanes (diphenylacetylenes) was in fact higher for the cyano terminated molecule (0.98 eV) than for the amine analogue (0.86 eV).[53] The lone pair of the CN group is essentially sp hybridised in character, whilst those of pyridine and aniline are sp^2 and sp^3 respectively. The increasing s character of the bonding can generally be considered to increase the stability of the lone pair in nitriles, decreasing the energy, which reduces the reactivity. This effect is commonly observed in coordination chemistry where cyano ligands, such as acetonitrile, are readily displaced by most other ligands. One possibility for the unexpectedly higher binding to gold could be related to the s orbital character of gold at the Fermi level, which may provide sufficient overlap with the sp nitrile orbital to form a strong bond.

Apart from N-based groups, other p-block elements can bind to gold through lone pair interactions. In a study by Park et.al. two thioether terminated compounds were examined to test the effect of restricting the orientation of the chalcogen atom lone pair.[93] The conductance of four molecules, 1,4-bis(methylthio)benzene, 2,3,6,7-tetrahydrobenzo[1,2-b:4,5-b′]dithiophene and their selenium analogues was measured using the STM-BJ method. In the cases of the tetrahydrodithiophene/selenophene compounds, the orientation of the lone pairs is fixed in the plane of the phenyl group pi-system, aiding overlap, whilst in the other two molecules, free rotation about

the Ph-S/Se bonds reduces the overlap. Park et.al. found that the conductance was slightly increased in the case of the two rigid molecules over the rotationally free compounds, which they explain through better overlap. Interestingly, practically no variation was found between the S and Se analogues. Phosphines have also been successfully used to form molecular junctions. Parameswaran et.al. tested a series of air-stable PPh_2 terminated alkanes finding a β value of 0.98 CH_2^{-1}.[94] The absolute conductance values were similar to the previously reported PMe_2 terminated molecules.[60]

A particularly good example of how the binding groups can influence the transport characteristics of the junction was demonstrated by Lee et.al. who showed that heat dissipation could be controlled by changing the anchor groups from isocyano to amino.[95] They proved that the sign of the slope of the transmission curve of a molecular junction governs in which electrode the majority of the heat is dissipated. They showed that the sign could be changed from positive for amino to negative for isocyano. This behaviour is related to the electron donating or accepting ability of the group, which places the HOMO closer to the Fermi level in the case of amino, but shifts the LUMO closer for the isocyano. Their results show that heat dissipation is directly related to the electronic structure of the junction, something which can easily be manipulated by the binding to the electrodes.

3.1.3 Direct gold-carbon binding

A recent development in the wiring of molecules to gold electrodes has been to explore the possibility of removing the dedicated terminal anchor group altogether. Cheng et al. have demonstrated the possibility of binding both ends of a carbon backbone to the electrodes, in effect forming a Au-C bond at each termini (Figure 11).[62] To do this they employed α,ω-functionalised bistrimethyltin compounds which, upon exposure to a gold surface, are thought to undergo trans-metallation in which the trimethyltin groups are replaced by atoms from the electrodes. Different backbones have been tested, the first being a series of alkanes ranging from butane to dodecane. The authors found that junctions could be formed with very high conductance, significantly higher than the corresponding thiol or amine terminated alkanes with identical numbers of carbon atoms. This result was based on the comparison of molecules with an identical number of CH_2 units, which means that the total length of the junctions being compared is quite different. If we compare junctions with like numbers of atoms from Au to Au, and consider the terminal carbons as *de facto* binding groups, then the direct binding is still more conducting, but the difference is reduced. We can also compare the conductance of the directly bonded alkanes with the alkanedithiols measured in reference [36], again on a like-numbered atom basis. Doing so we find that the thiols have a

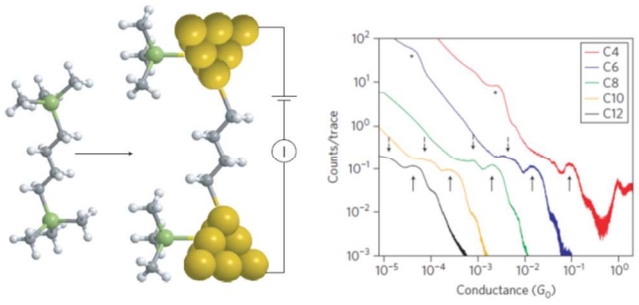

Figure 11. In situ cleavage of Me_3Sn terminated alkane to form direct Au-C bonds in molecular junctions. The histograms are for different length linear alkane chains from butyl (C4) to dodecyl (C12). Reprinted with permission from ref 62.

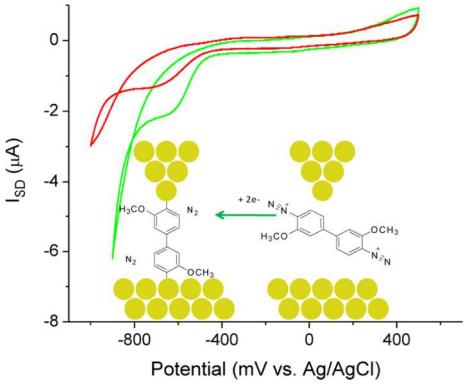

Figure 12. In situ reduction of bis-functionalized biphenyl diazonium salt. Reprinted with permission from ref 61.

conductance generally a factor 3-4 times lower than the directly bound alkane chains.

Another route to Au-C bond formation is through the use of diazonium salts. These are easily prepared from amines and are widely used in organic chemistry as electrophilic compounds for Suzuki coupling, azocoupling reactions, direct arylation on single wall carbon nanotube (SWNT)[96] and graphene.[97] More recently, they have been used in the direct functionalization of silicon[98] and, interestingly for transport measurements, using conductive materials such as gold or gold nanoparticles.[99] They are an appealing alternative to Au-C bond formation from tin derivatives as, apart from being much less toxic, they can be reacted under various conditions that may be useful depending on the particular device requirements. These methods include: spontaneously reduced by i) metal surface, ii) chemical reaction, iii) ultrasonication, iv) heating or v) through mechanical scratching. Recently, Pinson et al. have also developed a photochemical procedure for grafting diazonium salts onto many surfaces.[100] All of these reducing procedures lead to the formation of direct bond between aryl or alkyl compounds and the surface (although the aryl diazonium salts are more stable compared with the alkyl compounds). The potential, however, for multiple radical reactions to occur, especially if other electrochemically active groups are present, may limit the use of this chemistry for certain molecules.

Only a few examples of the application of diazonium chemistry in the formation of Au-C contacts within single molecule junctions have been demonstrated. A nice example is that of Ricci et.al. who studied the effect of exchanging the Au-S bond for a Au-C bond in junctions of a redox active osmium complexes.[101] The molecules contained a single $Os(bipyridine)_3$ complex tethered to the underlying gold surface through either a thiophenyl or phenyl unit. In these experiments, an STM tip was placed in close proximity to the surface, pre-functionalised with the respective molecules, and a tunnel barrier was maintained using a setpoint current of 1 nA. The measurements were carried out under electrochemical control using a four-electrode setup, which allows molecular levels to be shifted independently of the electrode Fermi level, gating the conductance. Peaks in the conductance versus overpotential (E, or gate potential) were observed, indicating transport through one, or a few, molecules. The peak maxima were ascribed to the levels of the Os comples, and their position (E_{max}) shifted depending on the tip-sample bias voltage (V_{bias}). They found similar positions of E_{max} for both the Au-S and the Au-C contacted molecules at the respective bias voltages, suggesting that varying the anchor group had little influence on the electron transport. The results were also similar to a previously reported $Os(bipy)_3$ complex tethered through a pyridine

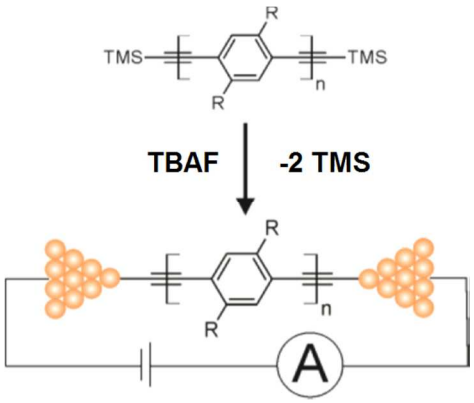

Figure 13. In situ cleavage of TMS-protected OPE molecules to form Au-C directly bonded molecular junctions. Reprinted with permission from ref 64.

group.[102] This behaviour suggests that, at least in these systems, the transport is not determined by the contact to the surface. It could be that the tunnel barrier between the tip and the molecule, which can be viewed as a very weak contact in comparison with the surface bond, dominates the conductance.

Another nice example is that of Hines et.al. who generated 2,2'-dimethoxy-4,4'-bis(diazonium)biphenyl in-situ within a breakjunction experiment (Figure 12).[61] By applying a sufficiently negative potential using an electrochemical gating electrode (-0.65 V versus Ag/AgCl), they cleaved the diazonium groups, and were able to form molecular junction bound by Au-C bonds on both sides of the biphenyl group. Comparing these junctions with a control species, 3,3'-dimethoxybenzidine (which binds through amine groups in the 4, 4' positions), they found similar values for the most probable conductance for both compounds. 2.3 x 10^{-3} G_0 was found for the Au-C bound compound, whilst 1.4 x 10^{-3} G_0 was seen for the amine bound species. This similarity in conductance was also observed by Cheng et.al. when they measured a single benzene ring directly bound to the electrodes. In this case the directly bound benzene and the 1,4-diaminobenzene analogue gave conductance values of 3 x 10^{-2} G_0 and 6 x 10^{-3} G_0 repectively.[62]

Considering the previous discussion, overall we thus find that the Au-C contact weakly modifies the conductance properties of single molecule junctions compared to thiol and amine anchors. Conversely, however, a recent report by Chen et.al. suggests that junctions of directly bound *p*-xylene (Au-CH_2-Ph-CH_2-Au) are significantly more conductive then the directly bound junctions of benzene (Au-Ph-Au).[103] This behaviour was in fact found for a series of polyphenyls contacted through Au-CH_2 bonds, where in fact the biphenyl derivative (CH_2-$(Ph)_2$-CH_2) conducts more than the 1,4-didehydrobenzene. To explain this result, the authors suggest that Au couples more effectively to the aryl pi-system through the methylene groups of *p*-xylene rather than when directly bound to the carbon atoms of benzene. In comparison to the directly bound *p*-xylene, the conductance of 1,4-benzenedimethanthiol was measured by Xiao et.al. and a value of 6 x 10^{-4} G_0 found as the most probable for a single molecule.[74] This is over three orders of magnitude lower than the same molecule without the S atoms as found by Chen et.al. This raises the question as to why the presence of S seems to reduce the conductance so dramatically. It would be good if an explanation could be derived from basic Chemistry principles. Hopefully, further experiments can shed some light into this phenomenon.

Another way to form Au-C bonds was demonstrated through the in-situ cleavage of terminal trimethylsilyl (TMS) protected alkynes. Hong et.al. prepared a range of TMS protected OPE derivatives with the general structure TMS-CC-Ph-CC-TMS (where CC indicates a triple bond) with between one, two and three phenylene ethynylene units (Figure 13).[64] Through the addition of two equivalents of tetrabutylammonium fluoride (TBAF) to the STM cell containing the relevant solution of TMS protected OPE, the authors found that the TMS was removed allowing molecular junctions to form. The presence of two TMS groups, one at each end of the molecule, was shown to be necessary as when only one alkyne group was protected by TMS, reaction with TBAF did not result in junctions being formed. To clarify the formation of the Au-C contact, Raman spectroscopy was carried out on gold surfaces modified with the OPE molecules capped with gold nanoparticles. Different signals were seen in the C-C triple bond region of the spectrum, and in particular a broad peak at 1950 cm^{-1}, which is roughly 200 cm^{-1} red-shifted compared to the free triple bond was found, in agreement with other reports of gold-alkynyl bonds.

3.2 Bidentate anchoring groups

There are fewer examples of single molecule studies using bidentate rather than monodentate anchor groups. Perhaps the most studied of such has been the carboxylic acid group (RCOOH). On Au(111) surfaces under electrochemical control, this group has been shown to adsorb via both oxygen atoms in an η-2 configuration, with the loss of the acidic proton.[104] This mode of binding may be expected to enhance the molecular coupling to the electrodes with respect to groups such as thiol and amine as two atoms can bind rather than only one. Several studies have investigated the transport properties of different length alkane chains terminated in carboxylic acids. In the first study, carried out by Chen et.al it was found that the conductance is in fact lower for the carboxylic acid than the respective amine and thiol molecules, when comparing the same number of carbon chain atoms (CH_2 groups).[65] In a separate study, Martin et.al measured the conductance of only carboxylic acid terminated alkanes,[89] which broadly agree with those of Chen, with some important differences. In the study of Chen, two groups of conductance values were found for COOH, as was the case for the thiol and amine compounds. In the study of Martin, only one group of values is mentioned for each molecule. The conductance Martin et.al found for hexanedioic acid (adipic acid, HOOC-$(CH_2)_4$-COOH) was 4x10^{-5} G_0, which agrees with the low conductance value

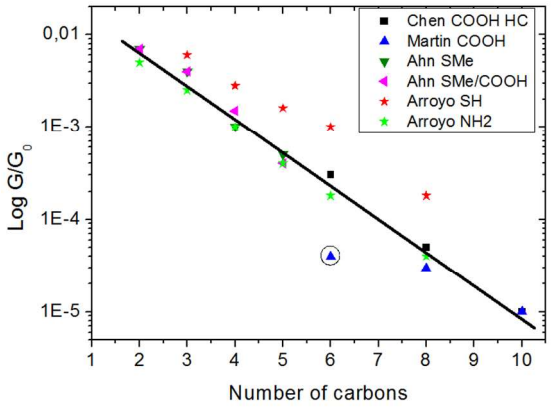

Figure 14. Comparison of the conductance values of various alkanes with different terminations showing the conductance as a function of the number of carbon atoms between the terminal hetero atoms. Plotted this way, the conductance values practically overlap for the COOH, SMe and NH_2 groups. A line is shown as a guide only. Thiols, however, are distinctly higher in conductance.

reported by Chen of $3x10^{-5}$ G_0. For octanedioic acid and decanedioic acid, however, the values reported by Martin are closer to the high conductance values of Chen. Whilst it is reassuring that similar value of conductance can be found by both groups using different techniques (Chen et.al. used the STM-BJ approach, whilst Martin et.al. used the non-conatct (I_s) method), this highlights a serious problem in how to compare results when different numbers of conductance groups are reported.

Ahn et.al. have measured a series of asymmetrically terminated alkane molecules using the STM-BJ technique.[66] They employed methylsulphide (R-SMe) contacts at one end, and COOH at the other. In control experiments, they showed that replacing the carboxyl group with an ester (RCOOMe) the conductance plateaus vanished, proving that binding occurs through deprotanation of the acid to form the carboxylate. They found that the asymmetrically terminated molecules had a lower conductance than the corresponding symmetric junctions containing only SMe contacts. They realised, however, that the COOH group adds an extra atom to the backbone of the molecule compared with the SMe group. When they compared the two sets counting the number of carbon atoms in the backbone, the conductance values in fact coincided. We have plotted the conductance values from the results of Chen, Martin and Ahn, along with our own data for amine and thiol terminated alkanes[36] in the following plot in Figure 14, counting the number of carbons in the backbone rather than the number of CH_2 groups.

Interestingly, all the values for the COOH, SMe and NH_2 contacted molecules fall practically on the same line (a line to guide the eye is shown in Figure 14). The values for the thiol terminated alkanes remain higher. We have, however, shown that alkanes have a tendency to aggregate in BJ experiments, which means that some degree of caution should be exercised when comparing the different compounds. Overall, the results point in the direction that the bidentate nature of the carboxyl group does not improve the conductance in comparison with monodentate groups.

Finally, we have composed a table which details the bond rupture forces for various binding groups discussed so far. This gives a sense of the relative bond strength to gold. We have chosen to quote the force rather than bond energy as it is this which is directly measured by experiment. The experiments are all made with a conducting atomic force microscope (cAFM) in which the BJ experiment can be perfomed whilst simultaneously monitoring the force. The values quoted are the mean values attributed to the final junction breakdown force, and hence represent an average over all junction geometries. The theoretical values are calculated from the derivative of the total energy curve calculated at different electrode-electrode spacings, where the maximum in the slope gives the breakdown force.

	Bond rupture force (nN)	
Anchor group	Experiment	Theory
R-S-Au	1.5 (R=CH_2)[a] 1.5 (R=CH_2)[c]	1.2 (R=Ph)[b] 2.2 (R=CH_2)[d] 1.5 (R=CH_2)[e]
R-SMe-Au (S coord)	0.5 (R=Ph)[f] 0.7 (R=CH_2)[g]	0.84 (R=CH_2)[g]
R-SH-Au (S coord)		0.6 (R=CH_2)[d]
R-NH_2-Au	0.53 (R=Ph)[h] 0.69 (R=CH_2)[h] 0.6 (R=CH_2)[g]	0.48 (R=Ph)[b] 1.0 (R=CH_2)[e] 0.46 (R=Ph)[h] 0.84 (R=CH_2)[h]
R-P($Ph)_2$-Au	0.8 (R=CH_2)[g]	
R-CN-Au		0.64 (R=Ph)[b]
R-NO_2-Au		0.32 (R=Ph)[b]
Pyridine-Au	0.8[h] 0.8[a] 0.55-0.63[i]	1.0[h]
Au-Au (chain)	1.5[j]	1.6[j]

Table 1. R is denoted as the main group attached to the anchor, not including the rest of the molecule. References: a,[105] b,[53] c,[81] d,[106] e (authors note it is the Au-Au bond which breaks, not the Au-S),[107] f,[108] g,[109] h,[85] i,[110] j.[80]

From table 1 we can see that all anchor groups, apart from the thiolate (RS-Au), have essentially a weaker bond to gold than an individual Au-Au bond within an atomic chain. Hence all groups would be expected to cleave at the Au-heteroatom bond, except the thiolate. Here the junction can be expected to break at an Au-Au bond, making chain formation more likely.[107] One interesting observation from this table is that for groups which have been tested attached to either phenyl or methylene units (i.e. to conjugated or non-conjugated units) there seems a tendency for the bond rupture force to be less for the conjugated phenyl molecules. As we discussed in section 3.1.2, there seems to be a relation between bond strength with known pKa values for these groups. The relation holds for phosphine and nitro groups, however, there is an anomaly when it comes to cyano. Here the bond rupture force is comparable to amines, whereas the basicity is significantly lower. This may indicate extra factors are involved, such a metal back donation, due to the pi-character and linear bond of the cyano group.

3.3 Larger multidentate anchoring groups.

3.3.1 Buckminsterfullerene (C_{60}):

In an attempt to move away from single bond contacts, which strongly influence the transport properties of molecular junctions, several groups have started investigating the possible benefits of using larger contacts between the molecule and the electrode. In particular, C_{60} have taken a prominent role in these studies, thanks mainly to the well-known synthetic strategies to place C_{60} at the termini of molecular wires. Pristine C_{60} has also been well studied on a variety of metallic surfaces, such as Ag,[111] Cu,[112] Pt[113] Pd[114] and Au[112] using scanning probe based techniques, providing detailed information about its different adsorption geometries and electronic structure through dI/dV spectra. The ability to study C_{60} in this way is advantageous over other atomic anchoring groups as we can use this information to understand the behviour of C_{60} as an anchor, and perhaps even make predictions.

Aside from the synthetic possibilities that C_{60} allows, the potential benefit of having a larger contact area to metal surfaces is that a more electronically transparent contact may be formed. The result of this would be, effectively, to move the principle transport barrier deeper into the molecule. The barrier would then depend on the structure of the molecule alone and not on the atomic details of the contact. Early studies seemed to suggest this was true, the first of which compared transport through 1,4-benzenedithiol, 1,4-benzenediamine and 1,4-bis(fullero[c]pyrrolidin-1-yl)benzene (BDC60) connected to gold using an MCBJ setup.[68] In this study, they compared the conductance properties of each molecular junction using a 2D histogram analysis. The conclusion of Martin et.al was that junctions with the fullerene anchors exhibited a lower

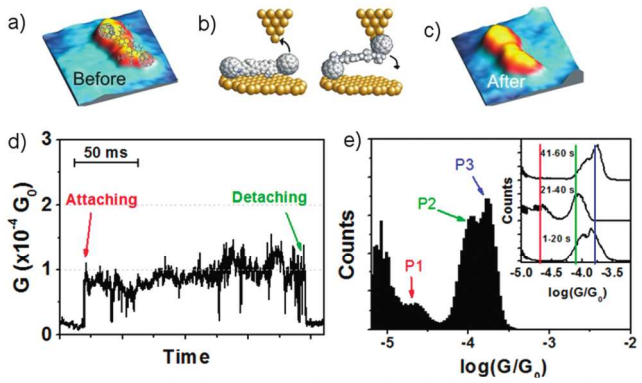

Figure 15. Targeted wiring approach. Reprinted with permission from ref 51.

spread of conductance values and could be stretched for longer times before cleavage. However, the study in fact found no well-defined conductance groups for either the amine or the thiol molecules. The region of conductance attributed to the fullerene-dumbbell junctions was also not as well defined as found for other compounds using the BJ technique.[9] Other groups have reported a lack of well-defined conductance features for 1,4-benzenedithiol,[76] but 1,4-benzenediamine has been shown to exhibit a well-defined conductance group, at least using the STM-BJ method.[115]

As previously discussed, rather than using the BJ technique to form molecular junctions, Leary et.al developed a new strategy to locate individual dumbbell molecules precisely on a gold surface and lift them with the tip of an STM.[51] To do this they first had to form a low coverage of molecules on the surface by drop casting from a very dilute solution of molecules. Individual molecules were imaged after leaving the sample a suitable length of time for the remaining solvent to dry. The method for wiring the molecules begins by placing the tip accurately above a molecule whilst maintaining a tunnelling current (Figure 15a). It is important to note that for this procedure to be successful, low drift is needed to keep the tip in the same position above the molecule for a long enough period. Here this is demonstrated by the *before* and *after* images in 15a and 15c showing about 1 nm drift per minute. The feedback loop of the microscope is temporarily disabled, and during this time jumps in current are recorded which correspond to attachment and detachment of the molecule with the tip, as seen in Figure 15d. Placing the tip to the side of the molecule resulted in no bridge formation. For the particular example shown, 60 seconds of data was recorded and compiled into a conductance histogram, shown in Figure 15e. The main result was that three peak could be seen, as labelled in 15e, spread over roughly an order of magnitude. This demonstrated that the molecule binds in several distinct ways inside the junction. As can be seen in the inset to 15e, where the data has been divided into three segments of 20 seconds, the ratio of the heights of the peaks changes during different periods of the measurement, indicating that the preferred binding fluctuates with time. The origin of this behaviour remains unknown, however, it was shown that deliberately varying the height of the tip above the molecule favoured different peaks (see Figure SI3 in ref[51]), which is a plausible explanation as tip height is difficult to control without the feedback loop engaged.

Leary et.al. also performed junction stretching experiments with a molecule wired to the tip. They found that the junctions could be stretched several Angstroms whilst maintaining a relatively constant conductance before breakdown. This showed that the molecule was well anchored to the electrodes, although the precise mode of binding at each end of the molecule is difficult to ascertain, and clearly varies during the measurement causing multiple conductance values.

Markussen et.al. carried out DFT calculations on the same molecule measured by Martin et.al and studied the effect of differing the surface coordination.[116] They compared the adsorption of a hexagon ring and a 5:6 bond (the bond between a hexagon and pentagon). They found that on Au(111), the conductance for both modes of adsorption was quite insensitive to translations of the molecule between different sites. However, a much larger difference was calculated between the hexagon and 5:6 binding modes. On the other hand, Bilan et.al. who have also studied the same molecule, calculated a large difference in transmission for different binding sites.[117] Rather than using flat electrodes, in their calculations pyramidal shaped clusters were used, terminating in either a single gold atom (top), or, by removing this atom, a triangle of three atoms (hollow). For comparison with the calculations of Markussen et.al. three Au atoms are bound to four C atoms in the hollow position, while in the top position, the apex gold atom is bound to two C atoms of a 6:6 bond. Bilan et.al. found that, despite the HOMO being pinned very close to the Fermi energy in both cases, the calculated conductance was 9.0×10^{-3} G_0 for the hollow position, whilst it was 2.5×10^{-6} G_0 for the top geometry. For pristine C_{60} junctions, a much lower variation in conductance was calculated using the same electrode shapes. For the top geometry, 0.55 G_0 was calculated, compared to 1.85 G_0 for the hollow. They attributed the sensitivity in the conductance of the dumbbell with electrode shape to the low effective phenyl-C_{60} coupling, which is the bottleneck in these junctions. This, they argued, made the transmission much more sensitive to energy level alignment and metal-molecule coupling. This is at odds with the calculations of Markussen et.al. and with the hypothesis we mentioned earlier. Bilan et.al. argued that the reason for this is that they have considered binding to undercoordinated gold atoms, and not to an extended surface as Markussen did. Thus, it appears that unless C_{60} can be reliably bound to a large number of atoms, a large conductance variation is theoretically expected.

Bilan et.al, also found a strong variation in the conductance of the dumbbell depending on the substitution of the central phenyl ring (Figure 16). This was different to their results of the 1,4-benzenedithiol and diamine analogues. They attributed this sensitivity to the narrow HOMO resonance in the dumbbell, which is weakly coupled to the electrodes. In the dithiol and diamine junctions, the HOMO (also the main conducting orbital) is much more strongly coupled to the electrodes, and is much broader as a consequence. This reduces the influence of changes in position of the HOMO due to substitution on the crossing of the transmission curve at the Fermi level. This carries an important message, that for successful chemical control of conductance one needs the relevant

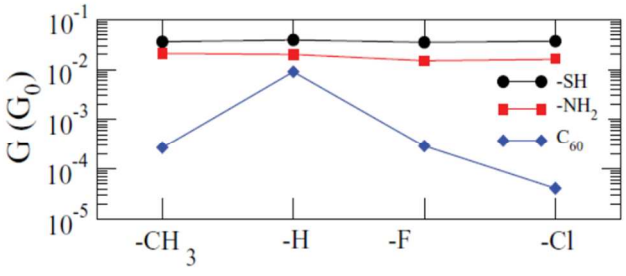

Figure 16. Theoretically calculated conductance values for various substituted benzenes with thiol, amine and C_{60} anchor groups. Reprinted with permission from ref 117.

molecular levels to be decoupled from the electrodes for a significant effect to be seen.

Gillemot et.al. showed that an individual dumbbell molecule could be successfully picked up using an STM tip and kept at the apex for a period of more than one hour.[118] This room temperature functionalization of an STM tip is interesting as it shows that junctions exposed to the ambient environment have the potential to be stable for far more than just a few seconds, which is the typical duration of a breakjunction experiment. In the experiment, the junction was not maintained for this period, the tip was moved up and down with respect to the surface, forming and breaking the molecular junction over the typical period of a second in order to understand its formation. During the experiment, however, the molecule moved very little on the tip, and as a result nearly the same junction was formed in each cycle. Thus it can be inferred that if the separation between the electrodes could have been kept fixed for the same period, the junction would have remained intact. Several other important aspects were highlighted by this experiment. The first being that to form the contact with surface, the layer of ambient adsorbates naturally present must be penetrated by the molecule, identified by an extra plateau in conductance as the molecule is approached. This highlights the non-trivial process of displacing other surface bound molecules using C_{60} anchor groups. The second point to be noted was that the conductance pathway through the molecule most likely bypassed one of the C_{60} groups, as suggested based on DTF calculations. It was predicted that the conductance across the two C_{60} should have been several orders of magnitude lower than experimentally observed. It is usually the case that calculated conductance values are higher than observed in experiments due to the well-known HOMO-LUMO gap underestimation of DTF and it was suggested, therefore, that the molecule was anchored to the tip in such a way that charge was being injected directly into the backbone. This phenomenon has been reported for other conjugated molecules, in particular oligoenes using methylsulfide anchor groups.[119]

Using C_{60} anchor groups, La Rosa et.al. showed that, aside from the electronic coupling between C_{60} and gold, it is possible to tune, albeit to a small degree, the coupling between the C_{60}s and the conjugated group between. This was achieved by studying spectroscopically the effect of changing the connecting group from a saturated pyrrolidine to a *quasi*-sp^2 hybridised cyclopropane.[120] Doing so resulted in a modest shift of the first two electrochemical reduction potentials by 20 mV to less negative potentials, and a slightly smaller π-π* gap indicating slightly better overall conjugation. In the same study, it was predicted that these effects should have a small, but noticeable, effect on the conductance, with the cyclopropane connection improving this by about a factor of three. As we have seen already, though, this effect is markedly smaller than the effect induced by changes in the C_{60}-electrode contact. This is further demonstrated in the following, final, section in which we focus on experiments carried out on pristine C_{60}.

3.3.2 Conductance properties of pristine C_{60}

To gain further insight into the nature of the Au-C_{60} interaction we shall now take a look at some of the experimental and theoretical results on pristine C_{60} adsorbed to various noble metal surfaces. There are several distinct ways in which C_{60} can bind to a metal surface which depend on its orientation. They are: i) through a single carbon atom, η^1, ii) to the centre of a hexagonal ring, η^6, iii) to the centre of pentagonal ring, η^5, iv) between a pentagon and a hexagon, η^2 v) between two hexagons, η^2. Carrying out tunnelling spectroscopy over the various faces of C_{60} it is possible to detect small changes in the energetic position of the LUMO relative to the gold Fermi level.[112] This level is closer to the Fermi level than the HOMO and is, therefore, the main transport level. As can be seen in Figure 17, the LUMO is located slightly below 1 V in the dI/dV spectrum on gold, indicating only a small amount of charge transfer takes place between the gold and the C_{60}. This level has been observed to shift depending on the surroundings of the molecule. Torrente et.al. found that within islands, the LUMO was located at 0.7 eV above the Fermi level, whilst this shifted upwards to 1.1 eV when the molecule is isolated.[121] It was argued that the more polarisable environment of the six neighbouring molecules in an island decreases the charging energy of the molecule relative to the isolated molecules.

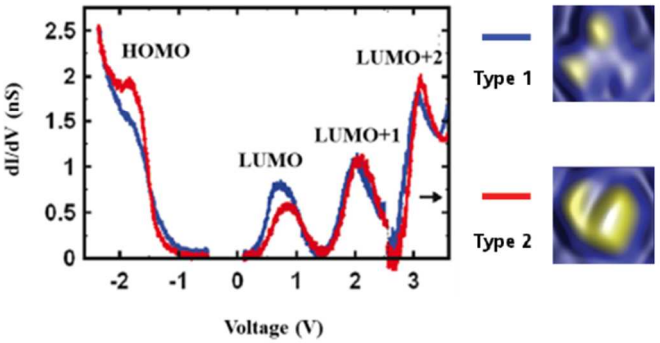

Figure 17. dI/dV curves taken above C_{60} molecules on Au(111) with different orientations. Reprinted with permission from ref 112.

Controlled contact to individual C_{60}s adsorbed on a copper surface was demonstrated by Neel et.al. using a low temperature STM.[122] As the tip was lowered towards individual molecules within a monolayer, an abrupt change from the slope due to vacuum tunnelling was found at around 0.25 G_0, which indicates the conductance at first contact to the molecule (Figure 18). By pressing the tip further, by several Angstroms, the authors found that the conductance increased to beyond $1G_0$, and distinct jumps in the conductance were seen. This provided evidence that the size of the contact to C_{60} influences the conductance. This was further elaborated in experiments carried out by Schull et.al. who generated differently sized clusters of Cu atoms on a Cu(111) surface to act as points of contact to a C_{60} which had been picked up by the tip. The

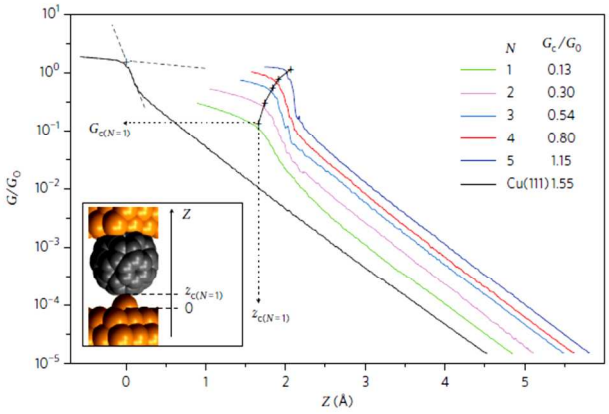

Figure 18. Conductance measurements of a single C_{60} molecule in contact with different size clusters of atoms on a copper surface. Reprinted with permission from ref 150.

size of these clusters ranged between one and five atoms, and the conductance on top of the bare surface was also compared. As can be seen in Figure 18, a positive correlation was found between the number of atoms in the surface contact and the conductance, which varied from 0.13 G_0 for the smallest contact to 1.15 for the largest. The conductance on the Cu (111) surface was even higher at 1.55 G_0. This work demonstrates very nicely that there is no unique molecular conductance value. Instead, the conductance is a delicate balance of the different possible bindings to the surface. The fact that changing the contact only on one side results in a one order of magnitude difference in conductance means that for a wire with two C_{60} groups, even more variability would be expected.

An important result with regards to using C_{60} and an anchoring group came from work carried out by Schull et.al. in which the conductance was measured two touching C_{60}s sandwiched between copper electrodes. By functionalising the STM tip with a single C_{60}, the molecule in fact becomes the tip, and it is then possible to re-image the surface and locate other C_{60} molecules. By placing the functionalised tip above a second molecule and approaching, the two molecules come into contact. This conductance at contact was found to be close to 10^{-2} G_0. This direct measurement of two C_{60}s highlights that the contacts in single dumbbell junctions will not be perfectly transmissive. This is already clear for gold by looking at the dI/dV spectra of C_{60} on Au(111) in Figure 17, and the results from Schull confirm the resistance of the C_{60} contact at least for Cu electrodes.

A further example of the sensitivity of C_{60} junctions to the contact came again from Schull et.al. by studying the conductance variation relative to the point of charge injection.[123] Contact conductance maps of C_{60} molecules and a Cu tip were compiled which allowed determination of the geometry of a single molecule junction at contact. They found that the conductance is determined by the hybridization of the p_z orbitals of the contacted C atoms with the orbitals of the tip apex atom. Thus C-C double (6:6) bonds were found to conduct better than single (5:6) bonds due to better orbital overlap.

The thermopower of molecular junctions consisting of one or two stacked molecules of C_{60} was measured by Evangelli et.al.[124] Thermopower is a result of a voltage difference between two electrodes due to heating of one of the electrodes. In a molecular junction, the sign and magnitude of the Seebeck coefficient (S) is controlled by the transmission profile at the Fermi level. The measurements showed that changes in conductance associated with changes in the contact between the C_{60} and the gold, resulted in changes in the thermopower. S was, however, always negative, meaning transport takes place through the LUMO. Interestingly, when two C_{60}s were stacked inside a junction, which was achieved by attaching one to the STM tip and lowering it onto another molecule, the thermopower increased approximately 100 % over the mono-C_{60} junctions. This shows the potential for manipulating thermopower perhaps through the use of multilayers. The conductance of these junctions was slightly lower than Schull et.al. measured using Cu electrodes, falling in the range of 10^{-3} G_0 for the gold electrodes, which agrees with the fact that the LUMO lies closer to the Fermi level on Cu than on Au.[112]

4. Electrode Material

Systematic studies of anchor group/electrode material combinations are important for testing our understanding of the roles played by Fermi level alignment, densities of states and charge transfer in single molecule junctions. In comparison to the number of studies, however, where the backbone of the molecule is the main focus, relatively few studies have looked at the effect of the electrode material. One such study by Ko et al. tested thiol and isothiocyanate anchored alkanes with Au, Pd and Pt via the breakjunction technique.[57] They concluded that the Pd-S junctions displayed the highest conductance followed by the Au-S junctions. The M-SCN junctions were all lower in conductance than the thiols in the order Pt-SCN>Pd-SCN>Au-SCN. They showed that the conductance followed the same trend as the bond order as calculated by a Mayer bond order analysis.

Kim et al. investigated a series of amine terminated oligophenyls with Au and Ag electrodes also using the MCBJ technique.[2] Compared to gold, silver electrodes were found to lower the molecular conductance due to the Fermi level lying further from the closest molecular levels. The beta value for the series was, however, found to be the same for both materials (both around 1.7 per phenylene unit). This behaviour was also noted by Ko et al. in the previous study using alkanes. From their theoretical analysis on the 1,4-benzenediamine molecule, both systems conduct via the molecular HOMO level, which is closer in the case of the Au-NH_2 system by roughly 0.3 eV. Interestingly, the Ag-NH_2 junctions have a higher apparent stretching distance than the Au-NH_2 junctions, which the authors attribute to a smaller initial gap formed by the Ag electrodes as the metallic junction breaks. This could possibly be rationalised by the fact that oxygen is seen to bond in the Ag junctions forming an intermediate Ag-O-Ag junction. This junction could reduce the snap-back of the electrodes. Silver is well known to tarnish under atmospheric conditions,[125] and although there is no direct evidence, a passivating oxide layer could interfere with the results by, for example, changing the density of states of the metal at the surface. In terms of conductance spread, the silver junctions gave a larger spread compared to the gold equivalents. This was traced to a greater sensitivity of the electronic coupling to the Ag-N-C bond angle.

If we return to the original hypothesis of using large groups as anchors to remove the unwanted contact-induced fluctuations, we can see that C_{60} on gold or copper is not going to work in this context. The experiments discussed in section 3.3.2 show that conductance is still sensitive to the precise atomic configuration of the contact, and as it is unlikely this can ever be controlled apart from at very low temperatures. Reducing conductance fluctuations by changing the metal is unlikely to work as all metals have a variable 3D structure in breakjunctions, although little work has been carried out with different metals to verify this. Other means to reduce the contact fluctuations must be sought. At present, however, there is no obvious solution.

The idea of using molecules as active elements in electrical devices implies that the dimensions of the electrodes must be small, in the 1-10 nm range, which clearly limits the size of the molecular contact. One potential way forward is perhaps through the use of planar contact arrangements which can be achieved by combining extended pi-systems with graphene electrodes.[4] Graphene is a 2D material which potentially offers benefits over 3D metal substrates in terms of the number of different contact geometries available to physisorbed species. Prins et al. used electroburing techniques to create graphene nanogaps onto which they adsorbed molecules with anthracene terminal groups designed to pi-stack to the graphene.[4] Molecules have been lifted with a gold tip from a graphene substrate.[126] Graphene can also be chemically modified through covalent anchoring of molecular wires, as has been shown by Guo et al.[127]

Garcia-Suarez et.al. have calculated that the position of the transmission resonances in planar junctions of pthalocyanine molecules adsorbed to graphene electrodes shift very little with respect to displacement of the electrodes.[128] Despite the profile at the Fermi level strongly depending on the adsorption site of the molecule, they argue that using a gate voltage to shift the transport resonances to the Fermi level would dramatically reduce the contact-induced fluctuations. This idea may work well for junctions is which the molecule acts purely as a wire, but at present it remains unclear how the conductance could be reliably gated. These ideas also pose considerable challenges from the experimental point of view, such as in the creation of well-defined graphene nano-electrodes and the subsequent challenge of placing only one molecule across the gap.

5. Theory of Single Molecule Junctions

We now turn to look at some advances in the theoretical understanding of single metal|molecule|metal junctions in order to gain some insight into the elements at play controlling single molecule transport. Current interest in transport at the nanoscale is not only due to the recently introduced experimental techniques discussed in section 2 of this review. Thanks to the availability of first-principles methods, normally based on density functional theory DFT in combination with nonequilibrium Green's function techniques, the electrical properties of single molecule junctions can now be modelled to a sophisticated degree.[129 130 131 132 133 134]

Firstly, it is well established that a combination of effects control the properties of single molecule junctions. These can be approximately divided into three groups: the intrinsic properties of the metal (the position of the Fermi Level, E_F and the density of states at E_F); the intrinsic properties of the molecule (the HOMO-LUMO gap, the molecular conformation and the bond characteristics, conjugated or saturated bonding); the properties of the interface (the metal-molecule bond angle, coordination site, bond dipole and interface states). Each of these properties can be seen to influence, to a certain extent, the alignment of the molecular levels with the metal states, which is, perhaps, the key concept to understand in single molecule transport. Herein lies one of the principle problems associated with metal-organic molecule interfaces. Indeed, it is the transport barrier, the energetic difference between the Fermi level of the electrodes and the molecular-based levels, which is relevant when discussing single molecule junctions. Using standard density functional theory (DFT), however, it is difficult to calculate level alignment accurately due to the well-known HOMO-LUMO gap underestimation, although recently various types of corrections have been suggested to overcome this problem.[135 136] Significantly, calculations on single molecule junctions also often assume particular binding geometries and symmetric, well defined, electrodes. This is no doubt an oversimplified picture of the real molecule/electrode geometry, as the experiment will effectively sample a wide range of geometries. Nevertheless, theoretical studies performed so far have clearly helped in understanding experimental results by providing information concerning the nature of the relevant orbitals, possible binding geometries and possible interference effects.

We have already discussed several nice pieces of theoretical work previously in this review and is often the cases that theory and experiment are intertwined and hence difficult to separate. We would like, however, to highlight some further relevant studies which provide additional insight into the role of the anchoring groups in single molecule junctions. This is by no means exhaustive, but our aim is simply to provide a flavour of the great efforts made by the theoretical community.

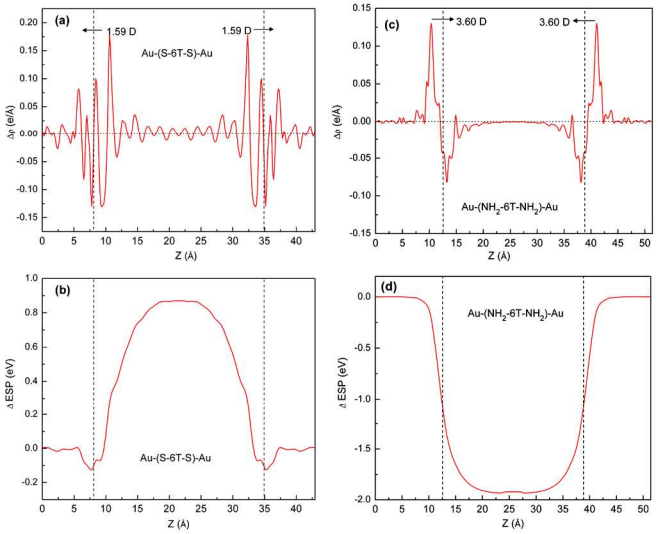

Figure 19. Plane-averaged charge density difference (a) and electrostatic potential difference (b) for Au-S-hexathiophene-S-Au. About 0.06*e* charge transfers from the Au electrode to the molecule resulting in a local dipole moment of 1.59 D developing at the interface. Vertical dashed lines indicate the interface positions. (c) plane-averaged electrostatic potential difference for Au-NH_2-hexathiophene-NH_2-Au. Charge transfer (~0.31*e*) occurs from the molecule to the Au electrode resulting in a local dipole moment of 3.60 D. Reprinted with permission from ref 138.

Seminario et.al. pointed out that the archetypal Au-S linkage may not be the best anchor group in terms of achieving optimal electronic transparency of the contact.[137] This is due to the fact that other metals present a high density of states (DOS) of s, p and d orbitals at the Fermi level (E_F) than gold does, and the Au-S bond also has an accute angle which is less favourable than linear bonding which has a degree of pi-character. For benzene, a large variation in transmission function line shape was found for different metal/anchor group combinations (group 10 and 11 metals were analysed along with thiol and cyano anchor groups). The most transmissive contact was found to be Pd-S thanks to the high DOS at E_F.

Peng et.al. have analysed several oligomeric systems, oligo(phenyl), oligo(thiophene) and oligo(pyrrole) with 1-6 rings, terminating in thiol anchor groups.[138] For the hexameric oligomers, in order to determine the band alignment of the molecular levels, the DOS was projected onto each oligomer unit (i.e. first, second and third rings). Firstly, for all three types of oligomer, the HOMO levels were the closest to the gold E_F, meaning transport should take place by hole-mediated tunnelling. In all cases, the states within the HOMO-LUMO gap are lowest on the rings farthest from the interface. These states can therefore be described as interface states as they are absent in the free molecule. By comparing the energy difference between the isolated molecular levels and the closest band edges for the molecular junction, the shift in the energy levels upon binding was found to be 0.6, 1.5 and 1.4 eV for the phenyl, thiophene and pyrrole respectively. This shift occurred towards the Fermi level, and suggests charge transfer from the metal electrodes to the molecule. This was verified by calculating the charge density difference between the molecule and the electrodes, which was found to be 0.07e, 0.06e and 0.06e to the molecule for the phenyl, thiophene and pyrrole respectively. The charge transfer induces a local dipole at the interface which will in turn change the electrostatic potential (ESP) of a junction. For sexithiophene, the results can be seen in figure 19a

and 19b, where the ESP changes by +0.9 eV at the centre of the molecule. This nicely explains the charge transfer and energy level shift upon binding of the molecule. Xue and Ratner also pointed out this behaviour in a previous study into the effects of the anchor group on the charge distribution across a molecular junction.[139]

To investigate how this behaviour is influenced by the nature of the anchoring group, Peng et.al. substituted the thiol for amine at the ends of the sexithiophene. Firstly, they found that instead of the HOMO lying closest to E_F as for the thiol terminated oligomer, the LUMO was closest for the amine analogue. To explain this change in alignment, the band alignment for isolated molecule and the molecule bound to the Au electrodes was calculated. The result was a downshift in the LUMO from 1.4 eV above E_F for the free molecule, to 0.15 eV above E_F for the bound molecule. This was shown to be a result of 0.3 electrons transferred from the molecule to the electrodes (figure 19c), i.e. in the opposite direction as the thiol analogue. The change in the ESP at the centre of the molecule is reversed compared to the thiol, being as large as -1.9 eV (figure 19d). Transfer of charge via a donor interaction for an aromatic amine adsorbed to gold has been verified experimentally by Kamenetska et al.[140]

In a separate study, Stadler and Jacobsen looked at level alignment in junctions of 4,4'-bipyridine and 4,4'-biphenyldithiol.[141] As in the study by Peng, they found that for the thiol, charge is transferred from the gold electrodes to the molecule, pushing the levels up in energy closer to E_F. On the other hand, for bipyridine, a net transfer of charge from the molecule to the electrodes was found, resulting in a lowering of the levels, placing the LUMO closest to E_F. Two effects were actually found to be at play in the bipyridine junctions. Apart from the transfer of charge to the electrodes, some charge was also found to move in the opposite direction to the molecular LUMO. This is expected if the LUMO approaches E_F, which partially stems the lowering of the LUMO. For bipyridine, the former effect was shown to dominate, whilst for biphenyl the filling of the LUMO dominates the charge transfer process.

It is intriguing that for the sexithiophene molecule, amine anchor groups are predicted to result in LUMO dominated transport. This is the opposite behaviour found for several aromatic amines, whose level alignment have been determined experimentally by thermopower measurements showing HOMO transport.[87] The message we can take from this result is that whilst the anchor group does strongly influence level alignment, the final position will also depend on the backbone of the molecule.

As we have already mentioned, the transport barrier is an important value to know in understanding transport characteristics. The fact that the molecular levels change significantly upon binding to a metal means the level positions derived from *ex-situ* spectroscopic methods are unreliable. This information must be obtained *in-situ*, and one method, which has been proposed to achieve this, is the so-called single-level model, which is also referred to as the resonant tunnelling model. [53] [142] [143] [144] The essence of the model is that information about the position of the closest molecular level and its coupling strength can be obtained from current-voltage (I/V) traces recorded on single molecule junctions. In the model certain assumptions are made to make it applicable to real experimental data: (i) that one level dominates the transport characteristics of a junction over the range of voltages (energies) studied; (ii) transport is phase coherent, that is there is no vibrational interaction between the electrons and the molecule. For details about the formulas used in this model, we refer the reader to other works where it is covered in full. It is sufficient to note that by fitting I/V traces with the model, it is possible to extract the level position (ε_0) and coupling strength (Γ), as has been done in several experimental studies.[53] [92] [145]

The single level model assumes that the level takes a Lorentzian line shape, which for most cases is a reasonable guess. However, recent theoretical work has shown that for particular molecules, the shape of the transmission curve at E_F is far from Lorentzian. This has been shown for molecules which display a phenomenon known as quantum interference (QI).[146] [147] Interference can potentially give rise to sharp transmission resonances which could form the basis of molecular switches with extremely high *On-Off* ratios.[148] Normally it is the structure of the molecule which determines if interference takes place, such as in cross-conjugated molecules or those with two weakly coupled degenerate states. What influence, therefore, do the anchor groups have in such molecules? Little evidence exists for a broad perspective on this question, however a recent study by Guédon et.al. has demonstrated that the choice of anchor group could be key in determining whether or not QI can be observed under experimental conditions.[149] They studied two sets of molecules that were either linearly conjugated (an oligophenylene ethynylene backbone) or cross-conjugated (based on an anthroquinone core). For both sets they studied molecules with two sulfur contacts at each end and molecules with only one sulfur contact. They found that the linearly conjugated molecules showed no QI, as did the cross-conjugated molecule with two sulfur contacts. Only the mono-sulfur contacted cross-conjugated molecule displayed evidence of QI. Theoretically, this was rationalised by arguing that the doubly-contacted molecule will have a different degree of charge transfer, and hence interfacial dipoles, compared to the mono-contacted molecule. As discussed before, this will result in a different level alignment in both cases, meaning only the mono-contacted molecule has the favourable level alignment within the experimental window for observation of QI. The important point here is that, as we have seen, the anchor groups control the level alignment within the junction, which means that they should be integral for the observation of QI effects.

6. Conclusions

Single molecule electronics has progressed greatly over the past decade. There are now many sophisticated experimental and theoretical tools at our disposal to probe molecular junctions as never before. One of the overriding conclusions from the past decade's work has been that anchor groups, and the way in which they interacts with the electrodes, dominate transport processes across the junction. We have witnessed a progression in the nature of the chemical groups used, starting from thiols, through various dative coordination groups such as amine, pyridine and methyl sulphide, to more recent attempts to improve the molecule-electrode coupling via Au-C bonds by metathesis or diazonium chemistry. One of the recurring problems, however, is that no matter which binding group we use, all the results tend to show fairly broad conductance distributions, at least an order of magnitude. This not only hinders the comparison between compounds, but also the likelihood of eventually building working devices operating via individual molecules. Attempts to reduce the variability are being made, but so far progress in this area is still lacking. Molecules with larger anchor groups like C_{60} when coupled to gold have also been found to give broad distributions, and this indicates that perhaps a complete rethinking of the interface is required for progress in the long term. We may turn to the use

of different electrode materials, in particular graphene, for which we have seen the first studies very recently.

In summary, the aforementioned results reveal that, despite the relatively wide number of chemically different anchor groups tested so far, more studies and new chemical species are needed to reach a better understanding of the critical role played by the chemical connectivity between the anchor groups and the metallic electrodes in single molecule conductance measurements. In this regard, only a systematic study at the nanometer scale together with the imagination of scientists should pave the way for the development of a rational and efficient molecular electronic devices.

Acknowledgements

This work has been supported by the MINECO of Spain (CTQ2011-24652), the European Research Council ERC-2012-ADG-20120216 (Chirallcarbon); Comunidad de Madrid (MADRISOLAR-2, S2009/PPQ-1533), the projects MAT2011-25046, RYC-2008-03328, and CSD2007-0010 (Consolider-ingenio, nanociencia molecular), the CAM through the project S2009/MAT-1726 (Nanobiomagnet) and the EU through the FP7 ITNs MOLESCO and FUNMOLS (project numbers 606728 and 212942, respectively) and ELFOS (FP7-ICT2009-6).

NM thanks the Alexander von Humboldt Foundation.

Notes and references

[a] IMDEA Nanociencia
C/Faraday 9, Campus Universitario de Cantoblanco, 28049 Madrid, Spain;
Tel: +34 91 299 87 89

[b] Departamento de Química Orgánica, Facultad de Ciencias Quiímicas, Universidad Complutense de Madrid, Ciudad Universitaria s/n, 28040, Madrid, Spain. Fax: +34 91-394-4103;
Tel: +34 91 394 4332

[c] Depto. Física de la Materia Condensada Mod. 3-610 – Universidad Autónoma de Madrid, 28049 Madrid, Spain;
Tel: +34 91 497 6196

† Footnotes should appear here. These might include comments relevant to but not central to the matter under discussion, limited experimental and spectral data, and crystallographic data.

Electronic Supplementary Information (ESI) available: [details of any supplementary information available should be included here]. See DOI: 10.1039/b000000x/

1. N. J. Kay, S. J. Higgins, J. O. Jeppesen, E. Leary, J. Lycoops, J. Ulstrup, and R. J. Nichols, *J. Am. Chem. Soc.*, 2012, **134**, 16817–16826.
2. T. Kim, H. Vázquez, M. S. Hybertsen, and L. Venkataraman, *Nano Lett.*, 2013, **13**, 3358–3364.
3. F. Chen, Z. Huang, and N. Tao, *Appl. Phys. Lett.*, 2007, **91**, 162106 – 162106–3.
4. F. Prins, A. Barreiro, J. W. Ruitenberg, J. S. Seldenthuis, N. Aliaga-Alcalde, L. M. K. Vandersypen, and H. S. J. van der Zant, *Nano Lett.*, 2011, **11**, 4607–4611.
5. J. He, F. Chen, J. Li, O. Sankey, Y. Terazono, C. Herrero, D. Gust, T. Moore, A. Moore, and S. Lindsay, *J. Am. Chem. Soc.*, 2005, **127**, 1384–1385.
6. B. Capozzi, E. J. Dell, T. C. Berkelbach, D. R. Reichman, L. Venkataraman, and L. M. Campos, *J. Am. Chem. Soc.*, 2014, **136**, 10486–10492.
7. W. Haiss, H. van Zalinge, D. Bethell, J. Ulstrup, D. Schiffrin, and R. Nichols, *Faraday Discuss.*, 2006, **131**, 253–264.
8. S. Martin, W. Haiss, S. J. Higgins, and R. J. Nichols, *Nano Lett.*, 2010, **10**, 2019–2023.
9. R. Huber, M. T. Gonzalez, S. Wu, M. Langer, S. Grunder, V. Horhoiu, M. Mayor, M. R. Bryce, C. Wang, R. Jitchati, C. Schoenenberger, and M. Calame, *J. Am. Chem. Soc.*, 2008, **130**, 1080–1084.
10. J. Ponce, C. R. Arroyo, S. Tatay, R. Frisenda, P. Gavina, D. Aravena, E. Ruiz, H. S. J. van der Zant, and E. Coronado, *J. Am. Chem. Soc.*, 2014, **136**, 8314–8322.
11. Z.-F. Liu, S. Wei, H. Yoon, O. Adak, I. Ponce, Y. Jiang, W.-D. Jang, L. M. Campos, L. Venkataraman, and J. B. Neaton, *Nano Lett.*, 2014, **14**, 5365–5370.
12. E. Leary, S. J. Higgins, H. van Zalinge, W. Haiss, R. J. Nichols, S. Nygaard, J. O. Jeppesen, and J. Ulstrup, *J. Am. Chem. Soc.*, 2008, **130**, 12204–12205.
13. H. B. Akkerman and B. de Boer, *J. Phys.-Condens. Matter*, 2008, **20**, 013001.
14. B. Xu and N. Tao, *Science*, 2003, **301**, 1221–1223.
15. W. Haiss, H. van Zalinge, S. Higgins, D. Bethell, H. Hobenreich, D. Schiffrin, and R. Nichols, *J. Am. Chem. Soc.*, 2003, **125**, 15294–15295.
16. X. Cui, A. Primak, X. Zarate, J. Tomfohr, O. Sankey, A. Moore, T. Moore, D. Gust, G. Harris, and S. Lindsay, *Science*, 2001, **294**, 571–574.
17. M. Reed, C. Zhou, C. Muller, T. Burgin, and J. Tour, *Science*, 1997, **278**, 252–254.
18. A. Nishikawa, J. Tobita, Y. Kato, S. Fujii, M. Suzuki, and M. Fujihira, *Nanotechnology*, 2007, **18**, 424005.
19. M. Teresa Gonzalez, E. Leary, R. Garcia, P. Verma, M. Angeles Herranz, G. Rubio-Bollinger, N. Martín, and N. Agrait, *J. Phys. Chem. C*, 2011, **115**, 17973–17978.
20. E. A. Della Pia, M. Elliott, D. D. Jones, and J. E. Macdonald, *ACS Nano*, 2012, **6**, 355–361.
21. L. Venkataraman, J. E. Klare, C. Nuckolls, M. S. Hybertsen, and M. L. Steigerwald, *Nature*, 2006, **442**, 904–907.
22. C. Li, A. Mishchenko, Z. Li, I. Pobelov, T. Wandlowski, X. Q. Li, F. Wuerthner, A. Bagrets, and F. Evers, *J. Phys.-Condens. Matter*, 2008, **20**, 374122.
23. E. Leary, H. Hobenreich, S. J. Higgins, H. van Zalinge, W. Haiss, R. J. Nichols, C. M. Finch, I. Grace, C. J. Lambert, R. McGrath, and J. Smerdon, *Phys. Rev. Lett.*, 2009, **102**, 086801.
24. V. Fatemi, M. Kamenetska, J. B. Neaton, and L. Venkataraman, *Nano Lett.*, 2011, **11**, 1988–1992.
25. J. Moreland and J. Ekin, *J. Appl. Phys.*, 1985, **58**, 3888–3895.
26. C. Zhou, C. Muller, M. Deshpande, J. Sleight, and M. Reed, *Appl. Phys. Lett.*, 1995, **67**, 1160–1162.
27. C. Muller, J. vanRuitenbeek, and L. Dejongh, *Phys. Rev.*

Lett., 1992, **69**, 140–143.
28. J. vanRuitenbeek, A. Alvarez, I. Pineyro, C. Grahmann, P. Joyez, M. Devoret, D. Esteve, and C. Urbina, *Rev. Sci. Instrum.*, 1996, **67**, 108–111.
29. C. Kergueris, J. Bourgoin, S. Palacin, D. Esteve, C. Urbina, M. Magoga, and C. Joachim, *Phys. Rev. B*, 1999, **59**, 12505–12513.
30. J. Reichert, R. Ochs, D. Beckmann, H. Weber, M. Mayor, and H. von Lohneysen, *Phys. Rev. Lett.*, 2002, **88**, 176804.
31. M. Teresa Gonzalez, A. Diaz, E. Leary, R. Garcia, M. Angeles Herranz, G. Rubio-Bollinger, N. Martín, and N. Agrait, *J. Am. Chem. Soc.*, 2013, **135**, 5420–5426.
32. W. Haiss, R. Nichols, H. van Zalinge, S. Higgins, D. Bethell, and D. Schiffrin, *Phys. Chem. Chem. Phys.*, 2004, **6**, 4330–4337.
33. W. Haiss, S. Martin, E. Leary, H. van Zalinge, S. J. Higgins, L. Bouffier, and R. J. Nichols, *J. Phys. Chem. C*, 2009, **113**, 5823–5833.
34. X. Li, J. He, J. Hihath, B. Xu, S. Lindsay, and N. Tao, *J. Am. Chem. Soc.*, 2006, **128**, 2135–2141.
35. C. Li, I. Pobelov, T. Wandlowski, A. Bagrets, A. Arnold, and F. Evers, *J. Am. Chem. Soc.*, 2008, **130**, 318–326.
36. C. R. Arroyo, E. Leary, A. Castellanos-Gomez, G. Rubio-Bollinger, M. Teresa Gonzalez, and N. Agrait, *J. Am. Chem. Soc.*, 2011, **133**, 14313–14319.
37. V. Kaliginedi, P. Moreno-Garcia, H. Valkenier, W. Hong, V. M. Garcia-Suarez, P. Buiter, J. L. H. Otten, J. C. Hummelen, C. J. Lambert, and T. Wandlowski, *J. Am. Chem. Soc.*, 2012, **134**, 5262–5275.
38. S. Martin, I. Grace, M. R. Bryce, C. Wang, R. Jitchati, A. S. Batsanov, S. J. Higgins, C. J. Lambert, and R. J. Nichols, *J. Am. Chem. Soc.*, 2010, **132**, 9157–9164.
39. R. Frisenda, M. L. Perrin, H. Valkenier, J. C. Hummelen, and H. S. J. van der Zant, *Phys. Status Solidi B-Basic Solid State Phys.*, 2013, **250**, 2431–2436.
40. L. Venkataraman, J. Klare, I. Tam, C. Nuckolls, M. Hybertsen, and M. Steigerwald, *Nano Lett.*, 2006, **6**, 458–462.
41. C. A. Martin, D. Ding, H. S. J. van der Zant, and J. M. van Ruitenbeek, *New J. Phys.*, 2008, **10**, 065008.
42. M. Tsutsui, K. Shoji, M. Taniguchi, and T. Kawai, *Nano Lett.*, 2008, **8**, 345–349.
43. T. Morita and S. Lindsay, *J. Am. Chem. Soc.*, 2007, **129**, 7262–7263.
44. C. Joachim, J. Gimzewski, R. Schlitter, and C. Chavy, *Phys. Rev. Lett.*, 1995, **74**, 2102–2105.
45. N. Neel, J. Kroeger, L. Limot, T. Frederiksen, M. Brandbyge, and R. Berndt, *Phys. Rev. Lett.*, 2007, **98**, 065502.
46. G. Schulze, K. J. Franke, A. Gagliardi, G. Romano, C. S. Lin, A. L. Rosa, T. A. Niehaus, T. Frauenheim, A. Di Carlo, A. Pecchia, and J. I. Pascual, *Phys. Rev. Lett.*, 2008, **100**, 136801.
47. L. Lafferentz, F. Ample, H. Yu, S. Hecht, C. Joachim, and L. Grill, *Science*, 2009, **323**, 1193–1197.
48. G. Reecht, F. Scheurer, V. Speisser, Y. J. Dappe, F. Mathevet, and G. Schull, *Phys. Rev. Lett.*, 2014, **112**, 047403.
49. C. Toher, R. Temirov, A. Greuling, F. Pump, M. Kaczmarski, G. Cuniberti, M. Rohlfing, and F. S. Tautz, *Phys. Rev. B*, 2011, **83**, 155402.
50. D. Kockmann, B. Poelsema, and H. J. W. Zandvliet, *Nano Lett.*, 2009, **9**, 1147–1151.
51. E. Leary, M. Teresa Gonzalez, C. van der Pol, M. R. Bryce, S. Filippone, N. Martín, G. Rubio-Bollinger, and N. Agrait, *Nano Lett.*, 2011, **11**, 2236–2241.
52. J. Heath and M. Ratner, *Phys. Today*, 2003, **56**, 43–49.
53. L. A. Zotti, T. Kirchner, J. C. Cuevas, F. Pauly, T. Huhn, E. Scheer, and A. Erbe, *Small*, 2010, **6**, 1529–1535.
54. M. Kamenetska, M. Koentopp, A. C. Whalley, Y. S. Park, M. L. Steigerwald, C. Nuckolls, M. S. Hybertsen, and L. Venkataraman, *Phys. Rev. Lett.*, 2009, **102**, 126803.
55. A. Mishchenko, L. A. Zotti, D. Vonlanthen, M. Buerkle, F. Pauly, J. Carlos Cuevas, M. Mayor, and T. Wandlowski, *J. Am. Chem. Soc.*, 2011, **133**, 184–187.
56. B. Kim, J. Beebe, Y. Jun, X. Zhu, and C. Frisbie, *J. Am. Chem. Soc.*, 2006, **128**, 4970–4971.
57. C.-H. Ko, M.-J. Huang, M.-D. Fu, and C. Chen, *J. Am. Chem. Soc.*, 2010, **132**, 756–764.
58. S. Yasuda, S. Yoshida, J. Sasaki, Y. Okutsu, T. Nakamura, A. Taninaka, O. Takeuchi, and H. Shigekawa, *J. Am. Chem. Soc.*, 2006, **128**, 7746–7747.
59. M. Kamenetska, S. Y. Quek, A. C. Whalley, M. L. Steigerwald, H. J. Choi, S. G. Louie, C. Nuckolls, M. S. Hybertsen, J. B. Neaton, and L. Venkataraman, *J. Am. Chem. Soc.*, 2010, **132**, 6817–6821.
60. Y. S. Park, A. C. Whalley, M. Kamenetska, M. L. Steigerwald, M. S. Hybertsen, C. Nuckolls, and L. Venkataraman, *J. Am. Chem. Soc.*, 2007, **129**, 15768–15769.
61. T. Hines, I. Diez-Perez, H. Nakamura, T. Shimazaki, Y. Asai, and N. Tao, *J. Am. Chem. Soc.*, 2013, **135**, 3319–3322.
62. Z.-L. Cheng, R. Skouta, H. Vazquez, J. R. Widawsky, S. Schneebeli, W. Chen, M. S. Hybertsen, R. Breslow, and L. Venkataraman, *Nat. Nanotechnol.*, 2011, **6**, 353–357.
63. D. Millar, L. Venkataraman, and L. H. Doerrer, *J. Phys. Chem. C*, 2007, **111**, 17635–17639.
64. W. Hong, H. Li, S.-X. Liu, Y. Fu, J. Li, V. Kaliginedi, S. Decurtins, and T. Wandlowski, *J. Am. Chem. Soc.*, 2012, **134**, 19425–19431.
65. F. Chen, X. Li, J. Hihath, Z. Huang, and N. Tao, *J. Am. Chem. Soc.*, 2006, **128**, 15874–15881.
66. S. Ahn, S. V. Aradhya, R. S. Klausen, B. Capozzi, X. Roy, M. L. Steigerwald, C. Nuckolls, and L. Venkataraman, *Phys. Chem. Chem. Phys.*, 2012, **14**, 13841–13845.
67. Z. Li, H. Li, S. Chen, T. Froehlich, C. Yi, C. Schönenberger, M. Calame, S. Decurtins, S.-X. Liu, and E. Borguet, *J. Am. Chem. Soc.*, 2014, **136**, 8867–8870.
68. C. A. Martin, D. Ding, J. K. Sorensen, T. Bjornholm, J. M. van Ruitenbeek, and H. S. J. van der Zant, *J. Am. Chem. Soc.*, 2008, **130**, 13198–13199.
69. J. Fock, J. K. Sorensen, E. Loertscher, T. Vosch, C. A. Martin, H. Riel, K. Kilsa, T. Bjornholm, and H. van der Zant, *Phys. Chem. Chem. Phys.*, 2011, **13**, 14325–14332.
70. J. Tour, L. Jones, D. Pearson, J. Lamba, T. Burgin, G.

Whitesides, D. Allara, A. Parikh, and S. Atre, *J. Am. Chem. Soc.*, 1995, **117**, 9529–9534.
71. M. Walter, J. Akola, O. Lopez-Acevedo, P. D. Jadzinsky, G. Calero, C. J. Ackerson, R. L. Whetten, H. Groenbeck, and H. Hakkinen, *Proc. Natl. Acad. Sci. U. S. A.*, 2008, **105**, 9157–9162.
72. O. Voznyy, J. J. Dubowski, J. T. Yates Jr., and P. Maksymovych, *J. Am. Chem. Soc.*, 2009, **131**, 12989–12993.
73. L. Dubois and R. Nuzzo, *Annu. Rev. Phys. Chem.*, 1992, **43**, 437–463.
74. X. Xiao, B. Xu, and N. Tao, *Nano Lett.*, 2004, **4**, 267–271.
75. W. Haiss, C. Wang, R. Jitchati, I. Grace, S. Martin, A. S. Batsanov, S. J. Higgins, M. R. Bryce, C. J. Lambert, P. S. Jensen, and R. J. Nichols, *J. Phys.-Condens. Matter*, 2008, **20**, 374119.
76. Y. Kim, T. Pietsch, A. Erbe, W. Belzig, and E. Scheer, *Nano Lett.*, 2011, **11**, 3734–3738.
77. J. Krans, J. van Ruitenbeek, V. Fisun, I. Yanson, and L. Dejongh, *Nature*, 1995, **375**, 767–769.
78. E. Leary, H. Van Zalinge, S. J. Higgins, R. J. Nichols, F. F. de Biani, P. Leoni, L. Marchetti, and P. Zanello, *Phys. Chem. Chem. Phys.*, 2009, **11**, 5198–5202.
79. M. T. Gonzalez, J. Brunner, R. Huber, S. Wu, C. Schoenenberger, and M. Calame, *New J. Phys.*, 2008, **10**, 065018.
80. G. Rubio-Bollinger, S. Bahn, N. Agrait, K. Jacobsen, and S. Vieira, *Phys. Rev. Lett.*, 2001, **87**, 026101.
81. C. Nef, P. L. T. M. Frederix, J. Brunner, C. Schoenenberger, and M. Calame, *Nanotechnology*, 2012, **23**, 365201.
82. J. R. Quinn, F. W. Foss Jr., L. Venkataraman, and R. Breslow, *J. Am. Chem. Soc.*, 2007, **129**, 12376–12377.
83. A. Salomon, D. Cahen, S. Lindsay, J. Tomfohr, V. Engelkes, and C. Frisbie, *Adv. Mater.*, 2003, **15**, 1881–1890.
84. M. S. Hybertsen, L. Venkataraman, J. E. Klare, A. C. Whalley, M. L. Steigerwald, and C. Nuckolls, *J. Phys.-Condens. Matter*, 2008, **20**, 374115.
85. M. Frei, S. V. Aradhya, M. Koentopp, M. S. Hybertsen, and L. Venkataraman, *Nano Lett.*, 2011, **11**, 1518–1523.
86. S. Y. Quek, M. Kamenetska, M. L. Steigerwald, H. J. Choi, S. G. Louie, M. S. Hybertsen, J. B. Neaton, and L. Venkataraman, *Nat. Nanotechnol.*, 2009, **4**, 230–234.
87. J. R. Widawsky, P. Darancet, J. B. Neaton, and L. Venkataraman, *Nano Lett.*, 2012, **12**, 354–358.
88. P. Reddy, S.-Y. Jang, R. A. Segalman, and A. Majumdar, *Science*, 2007, **315**, 1568–1571.
89. S. Martin, W. Haiss, S. Higgins, P. Cea, M. C. Lopez, and R. J. Nichols, *J. Phys. Chem. C*, 2008, **112**, 3941–3948.
90. P. Moreno-Garcia, M. Gulcur, D. Z. Manrique, T. Pope, W. Hong, V. Kaliginedi, C. Huang, A. S. Batsanov, M. R. Bryce, C. Lambert, and T. Wandlowski, *J. Am. Chem. Soc.*, 2013, **135**, 12228–12240.
91. K. A. Velizhanin, T. A. Zeidan, I. V. Alabugin, and S. Smirnov, *J. Phys. Chem. B*, 2010, **114**, 14189–14193.
92. B. M. Briechle, Y. Kim, P. Ehrenreich, A. Erbe, D. Sysoiev, T. Huhn, U. Groth, and E. Scheer, *Beilstein J. Nanotechnol.*, 2012, **3**, 798–808.
93. Y. S. Park, J. R. Widawsky, M. Kamenetska, M. L. Steigerwald, M. S. Hybertsen, C. Nuckolls, and L. Venkataraman, *J. Am. Chem. Soc.*, 2009, **131**, 10820–10821.
94. R. Parameswaran, J. R. Widawsky, H. Vazquez, Y. S. Park, B. M. Boardman, C. Nuckolls, M. L. Steigerwald, M. S. Hybertsen, and L. Venkataraman, *J. Phys. Chem. Lett.*, 2010, **1**, 2114–2119.
95. W. Lee, K. Kim, W. Jeong, L. Angela Zotti, F. Pauly, J. Carlos Cuevas, and P. Reddy, *Nature*, 2013, **498**, 209–212.
96. B. K. Price and J. M. Tour, *J. Am. Chem. Soc.*, 2006, **128**, 12899–12904.
97. L. Rodriguez-Perez, M. Angeles Herranz, and N. Martín, *Chem. Commun.*, 2013, **49**, 3721–3735.
98. X. Zhang, A. Tretjakov, M. Hovestaedt, G. Sun, V. Syritski, J. Reut, R. Volkmer, K. Hinrichs, and J. Rappich, *ACTA Biomater.*, 2013, **9**, 5838–5844.
99. L. Laurentius, S. R. Stoyanov, S. Gusarov, A. Kovalenko, R. Du, G. P. Lopinski, and M. T. McDermott, *ACS Nano*, 2011, **5**, 4219–4227.
100. M. Busson, A. Berisha, C. Combellas, F. Kanoufi, and J. Pinson, *Chem. Commun.*, 2011, **47**, 12631–12633.
101. A. M. Ricci, E. J. Calvo, S. Martin, and R. J. Nichols, *J. Am. Chem. Soc.*, 2010, **132**, 2494–2495.
102. T. Albrecht, K. Moth-Poulsen, J. Christensen, A. Guckian, T. Bjornholm, J. Vos, and J. Ulstrup, *Faraday Discuss.*, 2006, **131**, 265–279.
103. W. Chen, J. R. Widawsky, H. Vazquez, S. T. Schneebeli, M. S. Hybertsen, R. Breslow, and L. Venkataraman, *J. Am. Chem. Soc.*, 2011, **133**, 17160–17163.
104. S. Floate, M. Hosseini, M. Arshadi, D. Ritson, K. Young, and R. Nichols, *J. Electroanal. Chem.*, 2003, **542**, 67–74.
105. B. Xu, X. Xiao, and N. J. Tao, *J. Am. Chem. Soc.*, 2003, **125**, 16164–16165.
106. Y. Qi, J. Qin, G. Zhang, and T. Zhang, *J. Am. Chem. Soc.*, 2009, **131**, 16418–16422.
107. Y. Kim, T. J. Hellmuth, M. Bürkle, F. Pauly, and E. Scheer, *ACS Nano*, 2011, **5**, 4104–4111.
108. S. V. Aradhya, J. S. Meisner, M. Krikorian, S. Ahn, R. Parameswaran, M. L. Steigerwald, C. Nuckolls, and L. Venkataraman, *Nano Lett.*, 2012, **12**, 1643–1647.
109. M. Frei, S. V. Aradhya, M. S. Hybertsen, and L. Venkataraman, *J. Am. Chem. Soc.*, 2012, **134**, 4003–4006.
110. I. V. Pobelov, G. Mészáros, K. Yoshida, A. Mishchenko, M. Gulcur, M. R. Bryce, and Thomas Wandlowski, *J. Phys. Condens. Matter*, 2012, **24**, 164210.
111. X. Lu, M. Grobis, K. Khoo, S. Louie, and M. Crommie, *Phys. Rev. B*, 2004, **70**, 115418.
112. G. Schull, N. Neel, M. Becker, J. Kroeger, and R. Berndt, *New J. Phys.*, 2008, **10**, 065012.
113. C. Cepek, A. Goldoni, and S. Modesti, *Phys. Rev. B*, 1996, **53**, 7466–7472.
114. J. Weckesser, J. Barth, and K. Kern, *Phys. Rev. B*, 2001, **64**, 161403.
115. L. Venkataraman, Y. S. Park, A. C. Whalley, C.

Nuckolls, M. S. Hybertsen, and M. L. Steigerwald, *Nano Lett.*, 2007, **7**, 502–506.
116. T. Markussen, M. Settnes, and K. S. Thygesen, *J. Chem. Phys.*, 2011, **135**, 144104.
117. S. Bilan, L. A. Zotti, F. Pauly, and J. C. Cuevas, *Phys. Rev. B*, 2012, **85**, 205403.
118. K. Gillemot, C. Evangeli, E. Leary, A. La Rosa, M. T. González, S. Filippone, I. Grace, G. Rubio-Bollinger, J. Ferrer, N. Martín, C. J. Lambert, and N. Agraït, *Small*, 2013, **9**, 3812–3822.
119. J. S. Meisner, M. Kamenetska, M. Krikorian, M. L. Steigerwald, L. Venkataraman, and C. Nuckolls, *Nano Lett.*, 2011, **11**, 1575–1579.
120. A. La Rosa, K. Gillemot, E. Leary, C. Evangeli, M. Teresa Gonzalez, S. Filippone, G. Rubio-Bollinger, N. Agrait, C. J. Lambert, and N. Martín, *J. Org. Chem.*, 2014, **79**, 4871–4877.
121. I. F. Torrente, K. J. Franke, and J. I. Pascual, *J. Phys.-Condens. Matter*, 2008, **20**, 184001.
122. G. Schull, T. Frederiksen, M. Brandbyge, and R. Berndt, *Phys. Rev. Lett.*, 2009, **103**, 206803.
123. G. Schull, Y. J. Dappe, C. Gonzalez, H. Bulou, and R. Berndt, *Nano Lett.*, 2011, **11**, 3142–3146.
124. C. Evangeli, K. Gillemot, E. Leary, M. Teresa Gonzalez, G. Rubio-Bollinger, C. J. Lambert, and N. Agrait, *Nano Lett.*, 2013, **13**, 2141–2145.
125. C.R. Hammond, *The Elements, in Handbook of Chemistry and Physics 81st edition. CRC press*, 2000.
126. T. Kim, Z.-F. Liu, C. Lee, J. B. Neaton, and L. Venkataraman, *Proc. Natl. Acad. Sci.*, 2014, **111**, 10928–10932.
127. Y. Cao, S. Dong, S. Liu, L. He, L. Gan, X. Yu, M. L. Steigerwald, X. Wu, Z. Liu, and X. Guo, *Angew. Chem. Int. Ed.*, 2012, **51**, 12228–32.
128. V. M. Garcia-Suarez, R. Ferradas, D. Carrascal, and J. Ferrer, *Phys. Rev. B*, 2013, **87**, 235425.
129. F. Pauly, J. K. Viljas, U. Huniar, M. Haefner, S. Wohlthat, M. Buerkle, J. C. Cuevas, and G. Schoen, *New J. Phys.*, 2008, **10**, 125019.
130. A. Rocha, V. Garcia-Suarez, S. Bailey, C. Lambert, J. Ferrer, and S. Sanvito, *Phys. Rev. B*, 2006, **73**.
131. M. Brandbyge, J.-L. Mozos, P. Ordejón, J. Taylor, and K. Stokbro, *Phys Rev B*, 2002, **65**, 165401.
132. J. J. Palacios, A. J. Pérez-Jiménez, E. Louis, E. SanFabián, and J. A. Vergés, *Phys Rev B*, 2002, **66**, 035322.
133. Y. Xue, S. Datta, and M. A. Ratner, *J. Chem. Phys.*, 2001, **115**, 4292–4299.
134. K. S. Thygesen and K. W. Jacobsen, *Chem. Phys.*, 2005, **319**, 111 – 125.
135. C. Toher, A. Filippetti, S. Sanvito, and K. Burke, *Phys Rev Lett*, 2005, **95**, 146402.
136. P. Darancet, A. Ferretti, D. Mayou, and V. Olevano, *Phys Rev B*, 2007, **75**, 075102.
137. J. Seminario, C. De la Cruz, and P. Derosa, *J. Am. Chem. Soc.*, 2001, **123**, 5616–5617.
138. G. Peng, M. Strange, K. S. Thygesen, and M. Mavrikakis, *J. Phys. Chem. C*, 2009, **113**, 20967–20973.
139. Y. Xue and M. A. Ratner, *Phys Rev B*, 2004, **69**, 085403.
140. M. Kamenetska, M. Dell'Angela, J. R. Widawsky, G. Kladnik, A. Verdini, A. Cossaro, D. Cvetko, A. Morgante, and L. Venkataraman, *J. Phys. Chem. C*, 2011, **115**, 12625–12630.
141. R. Stadler and K. W. Jacobsen, *Phys. Rev. B*, 2006, **74**, 161405.
142. S Datta, *Electronic Transport in Mesoscopic Systems, Cambridge University Press, Cambridge*, UK, 1997.
143. L. Gruter, F. Cheng, T. Heikkila, M. Gonzalez, F. Diederich, C. Schonenberger, and M. Calame, *Nanotechnology*, 2005, **16**, 2143–2148.
144. E. H. Huisman, C. M. Guedon, B. J. van Wees, and S. J. van der Molen, *Nano Lett.*, 2009, **9**, 3909–3913.
145. Y. Kim, A. Garcia-Lekue, D. Sysoiev, T. Frederiksen, U. Groth, and E. Scheer, *Phys. Rev. Lett.*, 2012, **109**, 226801.
146. P. Sautet and C. Joachim, *Chem. Phys. Lett.*, 1988, **153**, 511–516.
147. D. Q. Andrews, G. C. Solomon, R. P. Van Duyne, and M. A. Ratner, *J. Am. Chem. Soc.*, 2008, **130**, 17309–17319.
148. L. A. Zotti, E. Leary, M. Soriano, J. Carlos Cuevas, and J. Jose Palacios, *J. Am. Chem. Soc.*, 2013, **135**, 2052–2055.
149. C. M. Guedon, H. Valkenier, T. Markussen, K. S. Thygesen, J. C. Hummelen, and S. J. van der Molen, *Nat. Nanotechnol.*, 2012, **7**, 304–308.
150. G. Schull, T. Frederiksen, A. Arnau, D. Sánchez-Portal, R. Berndt, *Nat. Nanotechnol.*, 2011 **6**, 23–27.
151. R. L. Whetten, R. C. Price, *Science*, 2007, **318**, 407–408.